Benzene Hydrogenation by Silica-Supported Catalysts Made of Palladium Nanoparticles and Electrostatically Immobilized Rhodium Single Sites

Pierluigi Barbaro,[†] Claudio Bianchini,*[,†] Vladimiro Dal Santo,[‡] Andrea Meli,[†] Simonetta Moneti,[†] Claudio Pirovano,[§] Rinaldo Psaro,*[,‡] Laura Sordelli,[‡] and Francesco Vizza[†]

ICCOM-CNR, Area di Ricerca CNR di Firenze, Via Madonna del Piano 10, 50019 Sesto Fiorentino, Firenze, Italy, ISTM-CNR, Via C. Golgi 19, 20133 Milano, Italy, and Dipartimento CIMA, Università degli Studi di Milano, Via G. Venezian 21, 20133 Milano, Italy

Received March 10, 2008

The complex [Rh(cod)(dppp)]OTf (Rh(cod)) has been immobilized onto silica-supported palladium nanoparticles (Pd/SiO_2) via a dual H-bond/ionic interaction (dppp = 1,3-bis(diphenylphosphino)propane; cod = cycloocta-1,5-diene). The product obtained, Rh(cod)-Pd/SiO_2, has been employed to catalyze the hydrogenation of benzene to cyclohexane, showing much higher activity as compared to Pd/SiO_2, while Rh(cod) grafted on bare silica ($Rh(cod)/SiO_2$) is totally inactive. The catalyst generated by Rh(cod)-Pd/SiO_2 exhibits a remarkable stability and can be recycled several times with no loss of activity, even if exposed to air. In situ and ex situ EXAFS and DRIFTS measurements, batch catalytic reactions under different conditions, deuterium labeling experiments, and model organometallic studies, taken altogether, have provided valuable mechanistic information. The reduction of benzene to cyclohexa-1,3-diene occurs with the cooperation of the two metals, while the rhodium single sites are more effective than the palladium nanoparticles in the hydrogenation of cyclohexa-1,3-diene to cyclohexane.

Introduction

Tethered complexes on supported metals (TCSM) constitute a particular class of hybrid catalysts that can be used in a number of heterogeneous processes such as arene hydrogenation,[1–4] hydrodefluorination of fluoroarenes,[5] alkene hydroformylation,[6] hydrodechlorination of chlorophenols,[7] and direct reduction of C═O functions to CH_2 without the intermediacy of carbynols.[8] While the supported metals are generally obtained by standard procedures, involving impregnation of porous oxides with metal salts followed by calcination/reduction, the immobilization of the metal complexes onto the support material has been so far achieved by three distinct methods: (a) Covalent grafting of a remote part of the ligand;[1,3,5,6] (b) H-bond grafting of a remote part of the ligand;[1,2] (c) sol–gel entrapment of both metal complexes and metal particles.[4,7,8] Simplified sketches of TCSM catalysts of the types a and b, containing palladium nanoparticles and Rh^I(cod) moieties (cod = cycloocta-1,5-diene) immobilized onto silica, are shown in Scheme 1.[1–3,5,6]

Scheme 1

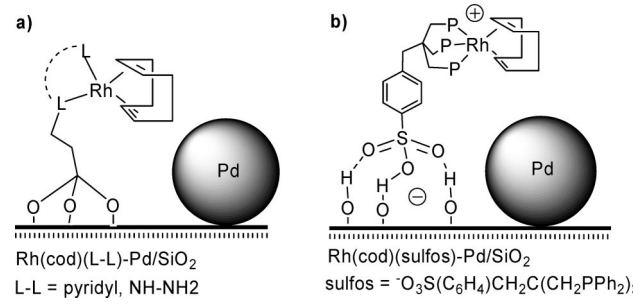

Rh(cod)(L-L)-Pd/SiO_2
L-L = pyridyl, NH-NH2

Rh(cod)(sulfos)-Pd/SiO_2
sulfos = $^-O_3S(C_6H_4)CH_2C(CH_2PPh_2)_3$

Irrespective of the preparation procedure and of the combination of metals, the known TCSM catalysts show higher activity in a number of hydrogenation reactions as compared to the separate components under comparable experimental conditions. Angelici proposed that the enhanced activity of TCSM catalysts may be due to a hydrogen spillover process,[9] promoted by the supported metallic phase, that would enhance specifically the activity of the molecular catalyst.[3] A study of the hydrogenation of arenes with a catalyst obtained by silica sol–gel coentrapment of metallic palladium and $[Rh(cod)(\mu\text{-}Cl)]_2$ disagreed with the

* To whom correspondence should be addressed. E-mail: claudio.bianchini@iccom.cnr.it.
† ICCOM-CNR.
‡ ISTM-CNR.
§ Dip. CIMA.

(1) Bianchini, C.; Meli, A.; Vizza, F. In *The Handbook of Homogeneous Hydrogenation*; de Vries, J. G., Elsevier, C. J., Eds.; Wiley-VCH: Weinheim, Germany, 2007; Vol. 1, pp 455–488.
(2) (a) Barbaro, P.; Bianchini, C.; Dal Santo, V.; Meli, A.; Moneti, S.; Psaro, R.; Scaffidi, A.; Sordelli, L.; Vizza, F. *J. Am. Chem. Soc.* **2006**, *128*, 7065. (b) Bianchini, C.; Dal Santo, V.; Meli, A.; Moneti, S.; Moreno, M.; Oberhauser, W.; Psaro, R.; Sordelli, L.; Vizza, F. *Angew. Chem., Int. Ed.* **2003**, *42*, 2636.
(3) (a) Yang, H.; Gao, H.; Angelici, R. J. *Organometallics* **2000**, *19*, 622. (b) Gao, H.; Angelici, R. J. *Organometallics* **1999**, *18*, 989. (c) Perera, M. A. D. N.; Angelici, R. J. *J. Mol. Catal. A: Chem.* **1999**, *149*, 99. (d) Gao, H.; Angelici, R. J. *J. Mol. Catal. A: Chem.* **1999**, *149*, 63. (e) Gao, H.; Angelici, R. J. *J. Mol. Catal. A: Chem.* **1999**, *145*, 83. (f) Gao, H.; Angelici, R. J. *New J. Chem.* **1999**, *23*, 633. (g) Gao, H.; Angelici, R. J. *J. Am. Chem. Soc.* **1997**, *119*, 6937.
(4) Abu-Reziq, R.; Avnir, D.; Miloslavski, I.; Schumann, H.; Blum, J. *J. Mol. Catal. A: Chem.* **2002**, *185*, 179.
(5) Yang, H.; Gao, H.; Angelici, R. J. *Organometallics* **1999**, *18*, 2285.
(6) Gao, H.; Angelici, R. J. *Organometallics* **1998**, *17*, 3063.
(7) (a) Bovkun, T. T.; Sasson, Y.; Blum, J. *J. Mol. Catal. A: Chem.* **2005**, *242*, 68. (b) Ghattas, A.; Abu-Reziq, R.; Avnir, D.; Blum, J. *Green Chem.* **2003**, *5*, 40.
(8) Abu-Reziq, R.; Avnir, D.; Blum, J. *J. Mol. Catal. A: Chem.* **2002**, *187*, 277.
(9) Delmon, B.; Fromont, G. F. *Catal. Rev. Sci. Eng.* **1996**, *38*, 69.

10.1021/om800223d CCC: $40.75 © 2008 American Chemical Society
Publication on Web 05/14/2008

Scheme 2

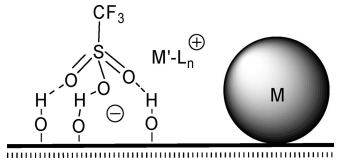

Scheme 3

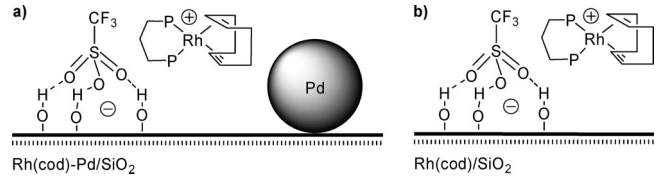

hydrogen spillover hypothesis and suggested that the action of both metals is caused by a sort of synergic effect for which no clear-cut explanation was provided, however.[4] The existence of a cooperative effect was later demonstrated and rationalized through an in-depth study of benzene hydrogenation to cyclohexane using the Rh^I-Pd^0 catalyst precursor Rh(cod)(sulfos)-Pd/SiO_2 shown in Scheme 1b.[2] It was proposed that the Rh^I single sites and the Pd^0 particles form a unique, stable entity throughout the catalytic cycle. Besides decreasing the extent of cyclohexa-1,3-diene disproportionation at palladium, the combined action of the two metals would activate the arene so as to allow the rhodium sites to enter the catalytic cycle and speed up the overall hydrogenation process by rapidly reducing benzene to cyclohexa-1,3-diene.

In this paper is reported a much simpler method to prepare TCSM catalysts, which can be extended to any cationic metal complex with no modification of the primitive molecular structure of the ligand, provided the counteranion is able to form H-bonds to the support material. To this purpose, an effective counteranion is the triflate ion ($CF_3SO_3^- = OTf^-$), as it contains up to three oxygen atoms suitable for H-bonding the surface hydroxyl groups of supports such as silica or alumina.[10b,11] The new procedure simply requires stirring a solution of a cationic metal complex bearing the triflate counteranion in the presence of silica-supported metal particles. It is noteworthy that the immobilization of the metal complex involves two different bonding interactions: the triflate ions form a net of H-bonds to the surface silanol groups of silica, thus generating a layer of negative charges, each of which attracts electrostatically the complex cation (Scheme 2).

The resulting H-bond/ionic immobilization of metal complexes is very robust in aprotic media and has been successfully applied to enantioselective hydrogenation reactions by chiral catalysts tethered to bare silica.[10b,11]

Herein, we specifically describe the synthesis and characterization of a new TSCM catalyst obtained by H-bond/ionic grafting the Rh^I complex [Rh(cod)(dppp)]OTf (Rh(cod)) to silica-supported palladium nanoparticles (Pd/SiO_2) (dppp = 1,3-bis(diphenylphosphino)propane). The product obtained, Rh(cod)-Pd/SiO_2 (Scheme 3a), has been employed to catalyze the hydrogenation of benzene to cyclohexane, showing much higher activity as compared to Pd/SiO_2, while Rh(cod) grafted on bare silica (Rh(cod)/SiO_2, Scheme 3b) was totally inactive.

The existence of a synergic action involving the rhodium single sites and the palladium particles has been proved and rationalized by means of in situ and ex situ EXAFS and DRIFTS measurements, batch catalytic reactions under different conditions, deuterium labeling experiments, and model organometallic reactions. In light of the results obtained, a reaction mechanism, containing a number of unusual intermediates as well as interactions between metal species and the support, is proposed.

Experimental Section

General Considerations. All reactions and manipulations were routinely performed under a nitrogen or argon atmosphere by using standard Schlenk techniques, unless stated otherwise. CH_2Cl_2 (impregnation procedures) was dried over molecular sieves under argon. Benzene and *n*-pentane (catalytic reactions) were distilled prior to use over Na and $LiAlH_4$, respectively. The rhodium complex [Rh(cod)(μ-Cl)]$_2$ was prepared as previously described.[12] All the other reagents and chemicals were reagent grade and were used as received from commercial suppliers. The Davison 332 (Grace) silica employed in this work was a high-surface-area hydrophilic mesoporous nonordered material. The support was ground, washed with 1 M HNO_3 and then with distilled water to neutrality, and dried overnight in an oven at 100 °C. The porosimetry and the surface area were determined by nitrogen adsorption. Nitrogen adsorption/desorption isotherms at liquid nitrogen temperature were measured on a Micromeritics ASAP 2010 instrument. All silica samples were routinely preoutgassed at 300 °C. The average pore radius (9.70 nm) and specific pore volume (1.43 cm^3/g) were calculated according to the Barret−Joyner−Halenda (BJH) theory.[13] The specific surface area (295 m^2/g) was obtained using the Brunauer–Emmett–Teller (BET) equation.[14] The palladium and rhodium contents in the tethered catalysts were determined by inductively coupled plasma atomic emission spectroscopy (ICP-AES) with a Intrepid Iris instrument (Thermo Elemental). Each sample (20–50 mg) was treated in a microwave-heated digestion bomb (Milestone, MLS-200) with concentrated HNO_3 (1.5 mL), 98% H_2SO_4 (2 mL), and a pellet (0.4 g) of a digestion aid reagent (0.1% Se in K_2SO_4). After the silica particles were filtered off, the solutions were analyzed. The addition of selenium was necessary to get an effective digestion of the phosphine ligand, which was hardly achievable by usual acid dissolution procedures. The same digestion method was employed to determine the metal contents in the products recovered after catalysis and in the organic solutions. Batch reactions under a controlled pressure of hydrogen were performed with a stainless steel Parr 4565 reactor (100 mL) equipped with a Parr 4842 temperature and pressure controller and a paddle stirrer. GC analyses of the solutions were performed on a Shimadzu GC-14 A gas chromatograph equipped with a flame ionization detector and a 30 m (0.25 mm i.d., 0.25 μm film thickness) SPB-1 Supelco fused silica capillary column. GC/MS analyses were performed on a Shimadzu QP5000 apparatus equipped with an identical capillary column. Deuterated solvents for NMR measurements (Aldrich) were dried over molecular sieves. ^1H (400.13 MHz), $^{13}C\{^1H\}$ (100.613 MHz), $^2H\{^1H\}$ (61.423 MHz), and $^{31}P\{^1H\}$ (161.98 MHz) NMR spectra were recorded on a Bruker Avance DRX-400 spectrometer equipped with a temperature controller accurate to ±0.1 °C. Chemical shifts are relative to external TMS (^1H

(10) (a) Bianchini, C.; Dal Santo, V.; Meli, A.; Moneti, S.; Moreno, M.; Oberhauser, W.; Psaro, R.; Soredelli, L.; Vizza, F. *J. Catal.* **2003**, *213*, 47. (b) Bianchini, C.; Barbaro, P.; Dal Santo, V.; Gobetto, R.; Meli, A.; Oberhauser, W.; Psaro, R.; Vizza, F. *Adv. Synth. Catal.* **2001**, *343*, 41. (c) Bianchini, C.; Dal Santo, V.; Meli, A.; Oberhauser, W.; Psaro, R.; Vizza, F. *Organometallics* **2000**, *19*, 2433. (d) Bianchini, C.; Burnaby, D. G.; Evans, J.; Frediani, P.; Meli, A.; Oberhauser, W.; Psaro, R.; Sordelli, L.; Vizza, F. *J. Am. Chem. Soc.* **1999**, *121*, 5961.

(11) (a) Raja, R.; Thomas, J. M.; Jones, M. D.; Johnson, B. F. G.; Vaughan, D. E. W. *J. Am. Chem. Soc.* **2003**, *125*, 14982. (b) de Rege, F. M.; Morita, D. K.; Ott, K. C.; Tumas, W.; Broene, R. D. *Chem. Commun.* **2000**, 1797.

(12) Bianchini, C.; Frediani, P.; Sernau, V. *Organometallics* **1995**, *14*, 5458.

(13) Barrett, E. P.; Joyner, L. G.; Halenda, P. P. *J. Am. Chem. Soc.* **1951**, *73*, 373.

(14) Brunauer, S.; Emmett, P. H.; Teller, E. *J. Am. Chem. Soc.* **1938**, *60*, 309.

and ^{13}C) or 85% H_3PO_4 (^{31}P) with downfield values reported as positive. The stereochemistry of the benzene hydrogenation was assessed by $^{13}C\{^1H\}$ and $^2H\{^1H\}$ NMR analysis of the reaction mixtures obtained by hydrogenation of C_6H_6-d_6 (ca. 80% conversion) with Pd/SiO_2 (1.93 wt % Pd) or Rh(cod)-Pd/SiO_2 (0.75–1.91 wt % Rh−Pd). Experimental $^{13}C\{^1H\}$ NMR spectra were computer simulated using the gNMR program.[15] ^1H (200.13 MHz) and $^{31}P\{^1H\}$ (81.01 MHz) high-pressure NMR (HPNMR) experiments were carried out on the Bruker ACP 200 instrument. The high-pressure 10 mm OD sapphire NMR tube was purchased from Saphikon (Milford, NH), while the titanium high-pressure charging head was constructed at the ICCOM-CNR.[16] *Note*: *Since high gas pressures are involved, safety precautions must be taken at all stages of studies involving high-pressure NMR tubes.* Elemental analyses (C, H, N) were performed using a Carlo Erba model 1106 elemental analyzer. Infrared spectra of molecular compounds were recorded on a Perkin-Elmer Spectrum BX FT-IR.

Preparation of Pd/SiO_2. Silica-supported palladium nanoparticles, usually 5 g batches (Pd content ranging from 1.66 to 2.08 wt %), were prepared from $PdCl_2/SiO_2$ by the following treatment: (1) calcination at 500 °C for 1 h in O_2 flow (40 mL/min) at a heating rate of 10 °C/min, followed by cooling in argon flow (40 mL/min) to room temperature; (2) reduction at 300 °C for 1 h in H_2 flow (40 mL/min) at a heating rate of 10 °C/min followed by cooling in argon flow (40 mL/min) to room temperature. $PdCl_2/SiO_2$ was, in turn, prepared by impregnation of 5 g of silica with a solution of $PdCl_2$ (0.14–0.18 g) in deionized water (50 mL) and 36% HCl (2 mL). The suspension was maintained under stirring for 4 h, and then the solvent was removed by evaporation under reduced pressure. The solid residue was washed with a small amount of water and dried under vacuum overnight.

Preparation of [Rh(cod)(dppp)]OTf (Rh(cod)). Solid AgOTf (0.11 g, 0.4 mmol) was added to a stirred solution of $[Rh(cod)(\mu\text{-}Cl)]_2$ (0.10 g, 0.2 mmol) and dppp (0.17 g, 0.4 mmol) in CH_2Cl_2 (20 mL). After 15 min, AgCl was eliminated by filtration and ethanol (50 mL) was added. Partial evaporation of the solvents under a steady stream of nitrogen gave yellow-orange crystals of Rh(cod) in 90% yield, which were collected by filtration and washed with ethanol and *n*-pentane. Anal. Calcd for $C_{36}H_{38}F_3O_3P_2RhS$ (772.60): C, 55.97; H, 4.96. Found: C, 55.70; H, 5.05. ^1H NMR (CD_2Cl_2, 20 °C): δ 7.5 (m, 20H, $P(C_6H_5)$), 4.62 (br s, 4H, CH cod), 2.72 (br s, 4H, CH_2 cod), 2.5 (br s, 4H CH_2 cod), 2.40 (m, 4H, PCH_2CH_2), 2.07 (m, 2H, PCH_2CH_2). $^{31}P\{^1H\}$ (CD_2Cl_2, 20 °C): δ 10.1 (d, J_{RhP} = 140 Hz).

In Situ HPNMR Study of the Reaction of Rh(cod) with H_2. A 10 mm sapphire tube was charged with a solution of Rh(cod) (0.05 g, 0.065 mmol) in THF-d_8 (2 mL) under nitrogen. After $^{31}P\{^1H\}$ and ^1H NMR spectra were recorded, the tube was pressurized with 30 bar of H_2 at room temperature. The reaction was followed at room temperature by $^{31}P\{^1H\}$ and ^1H NMR spectroscopy. Rh(cod) disappeared in 30 min with the formation of cyclooctane (coa) and several rhodium-dppp species, among which there was the bis-solvento complex $[Rh(solv)_2(dppp)]OTf$ (solv = THF, adventitious water; $^{31}P\{^1H\}$ NMR: δ 40.1 (d, J_{RhP} = 190.5 Hz); 35%).[17]

In Situ HPNMR Study of the Reaction of Rh(cod) with H_2 in the Presence of Benzene. Synthesis of $[Rh(\eta^6\text{-}C_6H_6)(dppp)]OTf$ ($Rh(C_6H_6)$). A 10 mm sapphire tube was charged with a THF-d_8 (2 mL) solution of Rh(cod) (0.05 g, 0.065 mmol) and a 10-fold excess of C_6H_6 under nitrogen. After $^{31}P\{^1H\}$ and ^1H NMR spectra were recorded, the tube was pressurized with 30 bar of H_2 at room temperature. The reaction was followed by variable-temperature $^{31}P\{^1H\}$ and ^1H NMR spectroscopy. At room temperature, Rh(cod) transformed selectively in 30 min into $Rh(C_6H_6)$, which was the only NMR-visible species at 40 °C for 1 h. The ^1H NMR spectrum showed the formation of coa, while no trace of benzene hydrogenated products was detected by GC/MS. Significant decomposition of $Rh(C_6H_6)$ occurred above 80 °C to give several unidentified products, among which, a hydride compound in a trace amount (^1H NMR multiplet at δ −22.71). However, no benzene hydrogenation occurred even at the latter temperature.

Preparation of $Rh(C_6H_6)$. A solution of Rh(cod) (0.40 g, 0.52 mmol) in a 3:1 (v/v) THF/benzene mixture (40 mL) was introduced by suction into a 100 mL Parr reactor previously evacuated by a vacuum pump. After pressurization with H_2 to 30 bar, the reaction mixture was stirred at room temperature for 30 min. Afterward, the reactor was depressurized and vented under a nitrogen stream and the contents were transferred into a Schlenk-type flask. Evaporating the solvent under vacuum gave $Rh(C_6H_6)$ as a yellow solid in 70% yield. Anal. Calcd (found) for $C_{34}H_{32}F_3O_3P_2RhS$ (742.53): C, 55.00; H 4.34. Found: C, 54.89; H 4.38. ^1H NMR (CD_2Cl_2, 20 °C): δ 7.48 (m, 20H, $P(C_6H_5)$), 6.01 (s, 6H, C_6H_6), 2.55 (m, 4H, PCH_2CH_2), 1.93 (m, 2H, PCH_2CH_2). $^{31}P\{^1H\}$ (CD_2Cl_2, 20 °C): δ 25.32 (d, J_{RhP} = 191.1 Hz).

Preparation of $[Rh(CO)_2(dppp)]OTf$ ($Rh(CO)_2$).[18] A solution of Rh(cod) (0.40 g, 0.52 mmol) in THF (40 mL) was introduced by suction into a 100 mL autoclave previously evacuated by a vacuum pump. After pressurization with 5 bar of CO, the reaction mixture was stirred for 30 min at room temperature. After the reactor was depressurized and vented under a nitrogen stream, the contents were transferred into a Schlenk-type flask. Evaporating the solvent under vacuum gave a yellow solid of $Rh(CO)_2$ (90% yield), which was washed with *n*-pentane. Anal. Calcd for $C_{30}H_{26}F_3O_5P_2RhS$ (720.44): C, 50.02; H 3.64. Found: C, 49.85; H 3.70. ^1H NMR (CD_2Cl_2, 20 °C): δ 7.48 (m, 20 H, $P(C_6H_5)$), 2.71 (m, 4H, PCH_2CH_2), 2.15 (m, 2H, PCH_2CH_2). $^{31}P\{^1H\}$ (CD_2Cl_2, 20 °C): δ 3.33 (d, J_{RhP} = 113 Hz). IR (KBr): ν_{CO} 2100, 2056 cm^{-1}.

Preparation of $[Rh(cod)(dppp)]OTf/SiO_2$ ($Rh(cod)/SiO_2$). Samples with rhodium contents spanning from 0.5 to 1.5 wt % were prepared following a known procedure.[10b] In particular, for catalysts with a metal loading of ca. 1 wt %, 1 g of pretreated silica was added to a stirred solution of 80 mg of Rh(cod) in 30 mL of anhydrous CH_2Cl_2 under argon. After 5 h, the grafted material was collected by filtration on a Pyrex Büchner filtering funnel under argon. The solid product was washed three times with 10 mL portions of anhydrous CH_2Cl_2 and kept under vacuum (10^{-6} bar) overnight at room temperature. The samples were stored under argon or nitrogen prior to use.

Preparation of $[Rh(cod)(dppp)]OTf\text{-}Pd/SiO_2$ ($Rh(cod)\text{-}Pd/SiO_2$). Samples of this bimetallic catalyst (0.07–1.07 wt % Rh and 1.58–1.91 wt % Pd) were prepared following a procedure analogous to that reported above for the silica-tethered Rh^I complex $Rh(cod)/SiO_2$ using, as support material, Pd/SiO_2, previously passivated under O_2 flow (40 mL/min) at room temperature for 30 min followed by flushing in argon flow (40 mL/min) for 30 min, instead of pretreated silica.

Preparation of $[Rh(\eta^6\text{-}C_6H_6)(dppp)]OTf/SiO_2$ ($Rh(C_6H_6)/SiO_2$). This compound (1.05 wt % Rh) was prepared following a procedure analogous to that reported above for $Rh(cod)/SiO_2$, using $Rh(C_6H_6)$ in place of Rh(cod) and a solvent mixture comprising anhydrous CH_2Cl_2 and benzene in a 4:1 (v/v) ratio.

Preparation of $[Rh(\eta^6\text{-}C_6H_6)(dppp)]OTf\text{-}Pd/SiO_2$ ($Rh(C_6H_6)\text{-}Pd/SiO_2$). This bimetallic compound (0.70 wt % Rh and 1.86 wt % Pd) was prepared following a procedure analogous to that reported above for $Rh(cod)\text{-}Pd/SiO_2$, using $Rh(C_6H_6)$ in place of Rh(cod) and a solvent mixture comprising anhydrous CH_2Cl_2 and benzene in a 4:1 (v/v) ratio.

(15) Budzelaar, P. H. M. *gNMR V4.0*; Cherwell Scientific Publishing: Oxford, 1995–1997 (Ivory Soft).

(16) Bianchini, C.; Meli, A.; Traversi, A. Ital. Pat. FI A000025, 1997.

(17) (a) Slack, D. A.; Greveling, I.; Baird, M. C. *Inorg. Chem.* **1979**, *18*, 3125. (b) Slack, D. A.; Baird, M. C. *J. Organomet. Chem.* **1977**, *142*, C69.

(18) Betley, T. A.; Peters, J. C. *Angew. Chem., Int. Ed.* **2003**, *42*, 2385.

Table 1. Best-Fit EXAFS Data at the Rh K-Edge[a]

entry	sample	shell	N	r (Å)	σ_{DW} (Å)	ΔE_0
1	Rh(cod)	C	4	2.213	0.09	2.7
		P	2	2.308	0.059	2
2	Rh(cod)/SiO_2 (0.71 wt % Rh)	C	4	2.057	0.064	3.2
		P	2	2.252	0.082	−4
3	Rh(cod)/SiO_2 (0.71 wt % Rh) heated in situ under H_2 (flow rate of 50 mL/min)up to 120 at 5 °C/min and then at 120 °C for 1 h	O	2.7	2.33	0.078	13
		P	2	2.26	0.063	6.6
4	Rh(cod)-Pd/SiO_2 (0.75–1.91 wt % Rh−Pd)	C	4	2.087	0.065	4
		P	2	2.246	0.091	−4
5	Rh(cod)-Pd/SiO_2 (0.75–1.91 wt % Rh−Pd) exposed to air at rt overnight	C	4	2.084	0.061	3.6
		P	2	2.251	0.078	−2.3
6	Rh(cod)-Pd/SiO_2 (0.75–1.91 wt % Rh−Pd) heated in situ under H_2 (flow rate of 50 mL/min) up to 120 at 5 °C/min and then at 120 °C for 1 h	P	2	2.275	0.073	0.2
		Pd	3.4	2.741	0.092	−2.6
7	Rh(cod)-Pd/SiO_2 (0.75–1.91 wt % Rh−Pd) after catalysis to 33% benzene conv.	C	6	2.088	0.086	5.9
		P	2	2.272	0.077	−1.7
		Pd	3.4	2.74	0.098	0
8	Rh(cod)-Pd/SiO_2 (0.75–1.91 wt % Rh−Pd) after catalysis to 33% benzene conv., exposure to air at rt overnight	O	2	1.98	0.069	1.7
		P	2	2.246	0.067	−1.7
		Pd	1.6	2.783	0.11	−1
9	Rh(cod)-Pd/SiO_2 (0.75–1.91 wt % Rh−Pd) after catalysis to 33% benzene conv. and exposure to air at rt overnight, catalysis to 68% benzene conv. (24 h)	C	4	2.07	0.068	0.7
		P	2	2.3	0.087	1.3
		Pd	3.8	2.655	0.099	−9

[a] Sample sealed inside sample holder under argon.

Table 2. Best-Fit EXAFS Data at the Pd K-Edge[a]

entry	sample	shell	N	r (Å)	σ_{DW} (Å)	ΔE_0	d_{mean} (Å)
1	Pd/SiO_2 (1.93 wt % Pd)	O	1.2	2.037	0.071	7.9	15
		Pd	6	2.722	0.079	−1.2	
2	Pd/SiO_2 (1.93 wt % Pd) exposed to O_2 flow at rt for 30 min	O	1.8	2.037	0.074	8.4	15
		Pd	6	2.718	0.081	2.5	
3	Pd/SiO_2 (1.93 wt % Pd) exposed to O_2 flow at rt for 30 min followed by wetting in CH_2Cl_2	O	1.4	2.037	0.063	7.9	18
		Pd	7.8	2.724	0.082	1	
4	Rh(cod)-Pd/SiO_2 (0.75–1.91 wt % Rh−Pd)	O	1.2	2.076	0.066	11	18
		Pd	7.9	2.723	0.087	8	
5	Rh(cod)-Pd/SiO_2 (0.75–1.91 wt % Rh−Pd) exposed to air at rt overnight	O	2	2.03	0.072	7.4	15
		Pd	5.7	2.715	0.098	0.6	
6	Rh(cod)-Pd/SiO_2 (0.75–1.91 wt % Rh−Pd) after catalysis to 33% benzene conv., exposed to air at rt overnight	O	1.8	2.04	0.068	8.4	15
		Pd	6	2.715	0.09	2.7	
7	Rh(cod)-Pd/SiO_2 (0.75–1.91 wt % Rh−Pd) after catalysis to 33% benzene conv. and exposure to air at rt overnight, catalysis to 68% benzene conv. (24 h)	Pd	9.5	2.725	0.9	1.4	30

[a] Sample sealed inside sample holder under argon.

Diffuse Reflectance Infrared Fourier Transform Spectroscopy (DRIFTS). Free and silica-supported metal complexes and their derivatives obtained after appropriate treatments, (i.e., ex situ catalytic runs, in situ reduction, etc.) were investigated by DRIFTS, using CO as probe molecule. The spectra were recorded on a FTS-60A spectrophotometer equipped with a homemade reaction chamber[19] and a online quadrupole mass spectrometer (HPR-20 QIC gas analysis mass spectrometer system/Hiden Analytical Ltd.). Unless otherwise stated, all samples were handled under an argon atmosphere in a drybox (water and oxygen levels below 0.1 ppm) containing a homemade reaction chamber, which was closed and connected to the gas lines of a gas-feeding apparatus. Before performing any CO chemisorption experiment, the samples were maintained under He. CO chemisorption was performed at the desired temperature for the desired time, followed by purging in He flow.

Extended X-ray Absorption Fine Structure Spectroscopy (EXAFS). Measurements were performed at the Rh and Pd K-edges on the samples reported in Tables 1 and 2. Palladium and rhodium foils were employed as reference standards for the extraction of the phase and amplitude experimental functions. The experiments were carried out at the XAFS beamline of the Elettra synchrotron in Trieste, with a double-crystal Si(311) monochromator and the ring operating at 2.4 GeV. The spectra were recorded in transmission mode, on samples sealed inside sample holders under a nitrogen atmosphere, at room temperature over a range of 1000 eV after the edge, with a sampling step of 2 eV and 2–4 s integration per point. Each spectrum was repeated three or four times for the signal-to-noise ratio optimization and for the error bars evaluation. The data analysis was performed with the FEFF7 software package.[20] Experimental $\chi(k)$ functions were extracted from the absorption spectra with a standard procedure and Fourier transformed over a k range 2.5–15 $Å^{-1}$. The main peaks of the Fourier transformed modulus were filtered and analyzed with a nonlinear least-squares fit program, which provided the atomic species, the number N of nearest neighbors, their distance R from the absorber atom, and the disorder σ_{DW} factor for each shell. The single scattering approximation was used in the theoretical signal modeling of the oxygen and palladium shells at the Rh K-edge. Multiple scattering was employed in the fitting procedure of the ligands bound to the rhodium atoms.

Heterogeneous Benzene Hydrogenation Reactions Using Rh-(cod)-Pd/SiO_2 as Catalyst Precursor. The autoclave was charged with the appropriate amount of a selected sample of Rh(cod)-Pd/SiO_2, the desired amount of benzene, and *n*-pentane (complement to 30 mL total volume). The ensemble was pressurized with H_2 to the desired pressure, heated to 40 °C, and then stirred at 1500 rpm. After 2 h, the autoclave was cooled to ambient temperature and depressurized. The liquid contents were analyzed by GC and GC/

(19) Dal Santo, V.; Dossi, C.; Fusi, A.; Psaro, R.; Mondelli, C.; Recchia, S. *Talanta* **2005**, *66*, 674.

(20) (a) Zabinsky, S. I.; Rehr, J. J.; Ankuninov, A.; Albers, R. C.; Eller, M. J. *Phys. Rev. B* **1995**, *52*, 2995. (b) Mustre de Leon, J.; Rehr, J. J.; Zabinsky, S. I.; Albers, R. C. *Phys. Rev. B* **1991**, *44*, 4146.

Table 3. Hydrogenation of Benzene to Cyclohexane Catalyzed by Rh(cod)-Pd/SiO_2: Dependence on the Rhodium Content[a]

entry	cat. precursor	cat. amnt (mg)	Pd wt %	Rh wt %	Pd μmol	Rh μmol	benzene (mL/mmol)	benzene/Pd ratio	benzene/Rh ratio	yield (%)[b]	TOF[c]	TOF_{Rh}[d]
1	Pd/SiO_2	47	1.93		8.5		0.430/4.818	565		3	72	
2	Rh(cod)-Pd/SiO_2	47	1.87	0.07	8.3	0.3	0.417/4.672	566	14616	21	491	1535
3	Rh(cod)-Pd/SiO_2	47	1.87	0.27	8.3	1.2	0.417/4.672	566	3789	23	537	436
4	Rh(cod)-Pd/SiO_2	47	1.91	0.75	8.4	3.4	0.426/4.773	566	1394	25	597	174
5	Rh(cod)-Pd/SiO_2	47	1.91	1.07	8.4	4.9	0.426/4.773	566	977	27	644	132
6	Rh(C_6H_6)-Pd/SiO_2	47	1.86	0.70	8.2	3.2	0.430/4.818	587	1507	35	843	264
7	Rh(cod)/SiO_2	47		0.65		3.0	0.430/4.818		1623	0	0	0
8	Rh(cod)-Pd/SiO_2	47	9.86	0.08	43.5	0.4	0.417/4.672	107	12789	36	841	2302
9	Rh(cod)-Pd/SiO_2	47	9.86	0.70	43.5	3.2	0.426/4.773	110	1493	52	1241	388

[a] Experimental conditions: *n*-pentane, complement to 30 mL total volume; H_2 pressure, 30 bar; temperature, 40 °C; time, 2 h; stirring rate, 1500 rpm. [b] Average values over at least three runs. [c] μmol of product h^{-1}. [d] mol of product (mol of Rh)$^{-1}$ h^{-1}.

Table 4. Hydrogenation of Benzene to Cyclohexane Catalyzed by Rh(cod)-Pd/SiO_2: Dependence on the Substrate Concentration, the Hydrogen Pressure, and the Catalyst Amount[a]

entry	cat. amnt (mg)	Pd wt %	Rh wt %	Pd μmol	Rh μmol	benzene (mL/mmol)	benzene/Pd ratio	benzene/Rh ratio	pH_2 (bar)	yield (%)[b]	TOF[c]	TOF_{Rh}[d]
1	47	1.59	1.00	7.0	4.6	0.430/4.818	686	1055	1.5	4	96	21
2	47	1.59	1.00	7.0	4.6	0.430/4.818	686	1055	5	12	289	63
3	47	1.59	1.00	7.0	4.6	0.430/4.818	686	1055	10	24	578	127
4	47	1.59	1.00	7.0	4.6	0.430/4.818	686	1055	16	27	650	142
5	47	1.59	1.00	7.0	4.6	0.430/4.818	686	1055	30	28	675	148
6	47	1.59	1.00	7.0	4.6	0.430/4.818	686	1055	48	38	915	200
7	47	1.59	1.00	7.0	4.6	0.860/9.636	1372	2110	30	26	1253	274
8	47	1.59	1.00	7.0	4.6	2.000/22.410	3191	4907	30	18	2017	442
9	47	1.59	1.00	7.0	4.6	4.000/44.821	6383	9814	30	13	2913	638
10	47	1.59	1.00	7.0	4.6	6.000/67.231	9574	14721	30	9.6	3227	707
11	47	1.59	1.00	7.0	4.6	8.000/89.641	12765	19628	30	7.4	3317	726
12	23	1.58	0.65	3.4	1.5	0.430/4.818	1411	3317	30	14	337	232
13	47	1.58	0.65	7.0	3.0	0.430/4.818	690	1623	30	27	650	219
14	94	1.58	0.65	14.0	5.9	0.430/4.818	345	812	30	57	1373	231

[a] Experimental conditions: *n*-pentane, complement to 30 mL total volume; temperature, 40 °C; time, 2 h; stirring rate, 1500 rpm. [b] Average values over at least three runs. [c] μmol of product h^{-1}. [d] mol of product (mol of Rh)$^{-1}$ h^{-1}.

Table 5. Hydrogenation of Benzene to Cyclohexane Catalyzed by Rh(cod)-Pd/SiO_2: Recycling Tests[a]

entry	run type	cat. amnt (mg)	Pd wt %	Rh wt %	Pd μmol	Rh μmol	benzene (mL/mmol)	benzene/Pd ratio	benzene/Rh ratio	yield (%)[b]	TOF[c]	TOF_{Rh}[d]
1	cycle	59	1.50	0.73	8.3	4.2	0.400/4.482	539	1071	27	605	145
2	recycle 1	59	1.50	0.73	8.3	4.2	0.400/4.482	539	1071	29	650	155
3	recycle 2	59	1.50	0.73	8.3	4.2	0.400/4.482	539	1071	32	717	171
4	recycle 3[e]	59	1.50	0.73	8.3	4.2	0.400/4.482	539	1071	41	919	220

[a] Experimental conditions: *n*-pentane, complement to 30 mL total volume; H_2 pressure, 30 bar; temperature, 40 °C; time, 2 h; stirring rate, 1500 rpm. [b] Average values over at least three runs. [c] μmol of product h^{-1}. [d] mol of product (mol of Rh)$^{-1}$ h^{-1}. [e] The catalyst recovered from recycle 2 was exposed to air for 2 days at room temperature before being employed in recycle 3.

MS. Catalytic data are reported in Tables 3 and 4. The stability of the immobilized catalyst against leaching from the support was established by recycling experiments (Table 5). To this purpose, after a catalytic run, the liquid phase was decanted under nitrogen in a drybox and the grafted rhodium/palladium product was washed with *n*-pentane until no trace of benzene or cyclohexane was detected by GC/MS in the decanted solvent (generally 3 × 20 mL). The residue was reused for a second run. After the liquid phase was analyzed by GC, the solvent was removed under reduced pressure and the residue was analyzed by both $^{31}P\{^1H\}$ NMR spectroscopy and ICP-AES. No trace of phosphorus was seen by NMR spectroscopy in all cases, while the amounts of rhodium detected by ICP-AES were <1 ppm. For comparative purposes, some hydrogenation reactions were also carried out using Pd/SiO_2, Rh(cod)/SiO_2, Rh(C_6H_6)/SiO_2, and Rh(C_6H_6)-Pd/SiO_2 as catalyst precursors (Table 3) as well as cyclohexa-1,3-diene and cyclohexene as substrates (Table 6).

Results and Discussion

Synthesis of Rhodium Complexes and Silica-Supported Catalyst Precursors. The preparation and characterization of Pd/SiO_2 with different metal contents have been described in a previous paper.[2] In this work, only samples with Pd contents of ca. 2 wt % have been used for both spectroscopic studies and catalytic reactions. EXAFS (Table 2, entry 1) and HRTEM[2] analyses showed these samples to contain highly dispersed palladium nanoparticles (mean diameter of ca. 15 Å). Rh(cod)/SiO_2 (0.71 wt % Rh) and Rh(cod)-Pd/SiO_2 (0.07–1.07 wt % Rh and 1.58–1.91 wt % Pd) are new compounds (Scheme 3), yet the synthetic procedure to either species closely resembles that developed to anchor cationic Rh^I-diphosphine complexes with triflate counteranions.[10b,11] The heterogenization of Rh(cod) was achieved by stirring a solution of this cationic complex in anhydrous CH_2Cl_2 in the presence of either bare silica or Pd/SiO_2. Following this simple procedure, the triflate anions get anchored to the surface silanol groups of silica via H-bonding, while the complex cations are kept close to the functionalized silica by ionic interaction. Provided the use of the resulting material in aprotic solvents, the overall support−anions−cations interaction is quite robust and no leaching has been ever observed even under harsh catalytic reactions.[10b,11] The only precaution required to prepare the hybrid material Rh(cod)-Pd/SiO_2 is to mildly passivate Pd/SiO_2 with oxygen so as to avoid any undesired chemical interaction of the palladium particles

Table 6. Hydrogenation of Cyclohexa-1,3-diene and Cyclohexene by Miscellaneous Catalysts[a]

entry	cat. precursor	cat. amnt (mg)	Pd wt %	Rh wt %	Pd μmol	Rh μmol	substrate[b]	substrate/Pd ratio	substrate/Rh ratio	B %[bc]	HDE %[b,c]	HE %[bc]	HA %[bc]	TOF_{Pd}[d]	TOF_{Rh}[d]
1	Pd/SiO_2	58	2.00		10.9		HDE	963		4		30	66	3851	
2	$Rh(cod)/SiO_2$	33		0.72		2.3	HDE		4546			4	96		18 183
3	$Rh(cod)$-Pd/SiO_2	60	1.94	0.39	10.9	2.3	HDE	960	4616	5			95	3838	18 463
4	Pd/SiO_2[e]	58	2.00		10.9		HDE	963		7	86	7		539	
5	Pd/SiO_2	58	2.00		10.9		HE	963				2	98	3774	
6	$Rh(cod)/SiO_2$	33		0.72		2.3	HE		4546			72	18		3273
7	$Rh(cod)$-Pd/SiO_2	60	1.94	0.39	10.9	2.3	HE	960	4616				100	3838	18 463

[a] Experimental conditions: substrate, 10.495 mmol (cyclohexa-1,3-diene, 1.00 mL; cyclohexene; 1.05 mL); *n*-pentane, complement to 30 mL total volume; H_2 pressure, 30 bar; temperature, 40 °C; time, 15 min; stirring rate, 1500 rpm. [b] B = benzene, HDE = cyclohexa-1,3-diene, HE = cyclohexene, HA = cyclohexane. [c] Average values over at least three runs. [d] mol of total product (mol of M)$^{-1}$ h^{-1}. [e] Under nitrogen.

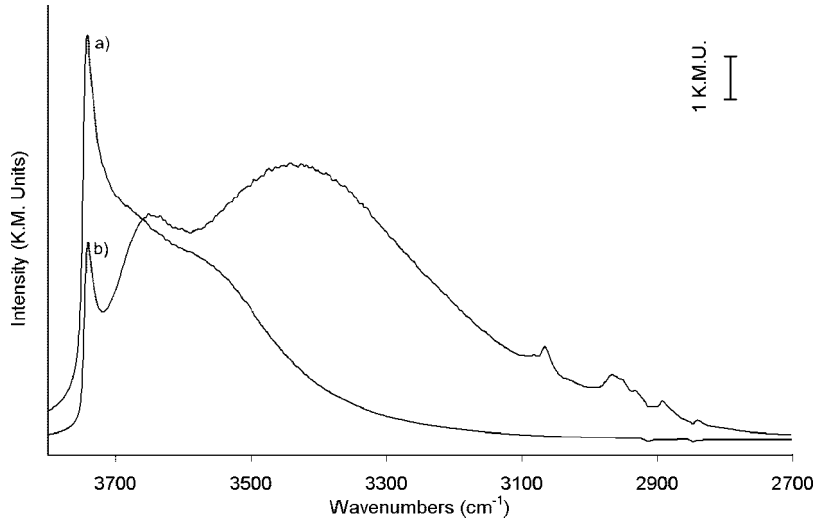

Figure 1. DRIFTS spectra, in the O−H stretching region, of (a) Pd/SiO_2 (1.93 wt % Pd) and (b) $Rh(cod)$-Pd/SiO_2 (0.75–1.91 wt % Rh−Pd).

with the impregnation solvent.[2a,21] The thin layer of surface oxide is readily removed by treatment with H_2. At variance with the TMCS catalysts obtained with the methods illustrated in Scheme 1, the complex cations in $Rh(cod)$-Pd/SiO_2 have a much higher degree of freedom, as their only constraint is to lie in proximity of the anions, which in turn can walk over the support by making and cleaving H-bonds.[10b,11]

Consistent with the H-bond anchoring of the triflate anions, the DRIFTS spectrum of $Rh(cod)$-Pd/SiO_2 (0.75–1.91 wt % Rh−Pd) showed a strong decrease in the intensity of the isolated silanols band at 3740 cm^{-1}, as compared to Pd/SiO_2 (1.93 wt % Pd), together with the occurrence of a broad band centered at ca. 3440 cm^{-1} due to the silanols in H-bond interaction with the sulfonate tail of the triflate groups (Figure 1).

Others detectable bands (C−H stretching of the dppp phenyls and of the cod ligand) showed only minor changes as compared to those of unsupported Rh(cod), suggesting that the structure of the rhodium complex remains unchanged after its grafting.

EXAFS Characterization of Rhodium Complexes and Silica-Supported Catalyst Precursors. Figure 2 shows the Fourier spectra at the Rh K-edge of Rh(cod), $Rh(cod)/SiO_2$ (0.71 wt % Rh), and $Rh(cod)$-Pd/SiO_2 (0.75–1.91 wt % Rh−Pd), while the Fourier spectra at the Pd K-edge of $Rh(cod)$-Pd/SiO_2 (0.75–1.91 wt % Rh−Pd) and Pd/SiO_2 (1.93 wt % Pd) are reported in Figure 3. Figures 2 and 3 show also the spectra of materials recovered after various treatments of Pd/SiO_2, $Rh(cod)/SiO_2$, and $Rh(cod)$-Pd/SiO_2. The spectra are not phase-corrected. The results of the spherical wave curve fitting analysis of the local surroundings of the absorbing atom, performed by least-squares refinement, are reported in Tables 1 and 2.

The main peak in the spectrum of Rh(cod) at the Rh K-edge consists of four carbon atoms from the cod ligand and two phosphorus atoms from dppp (Table 1, entry 1). The average Rh−P distance of 2.308 Å is comparable to that (2.315_{av} Å) obtained by a single-crystal X-ray diffraction analysis of the hexafluorophosphate derivative $[Rh(cod)(dppp)]PF_6$, while the average Rh−C distance of 2.213 Å is slightly shorter (2.250_{av} Å).[22] The same coordinative environment around the rhodium atom has been determined for $Rh(cod)/SiO_2$ (0.71 wt % Rh), which confirms that the present way of anchoring Rh(cod) onto silica fully preserves the structure of the complex cation (Table 1, entry 2). The only difference observed upon immobilization of Rh(cod) was the shortening of the Rh−C distances (2.057 Å), which may be an artifact of the EXAFS measurement, as the standard Gaussian description of the radial pair distribution underestimates distances in the presence of a high conformational disorder. Indeed, the electrostatically tethered complex cation $[Rh(cod)(dppp)]^+$ is expected to exhibit a higher degree of freedom as compared to the same cation packed in the crystal lattice of Rh(cod).[10b,11] The damping of the signal from C shells belonging to the PPh_2 groups can be due to the high σ_{DW} factor for the carbon atoms at distances greater than 3 Å, which reflects their thermal and conformational disorder. Exactly the same local structure, i.e., four equidistant C atoms and two phosphorus atoms (Table 1, entry 4), was found for the complex cation in $Rh(cod)$-Pd/SiO_2 (0.75–1.91 wt % Rh−Pd). No additional

(21) Solymosi, F.; Rasko, J. *J. Catal.* **1995**, *155*, 74.

(22) Kempe, R.; Spannenberg, A.; Heller, D. *Z. Kristallogr.–New Cryst. Struct.* **2001**, *216*, 153.

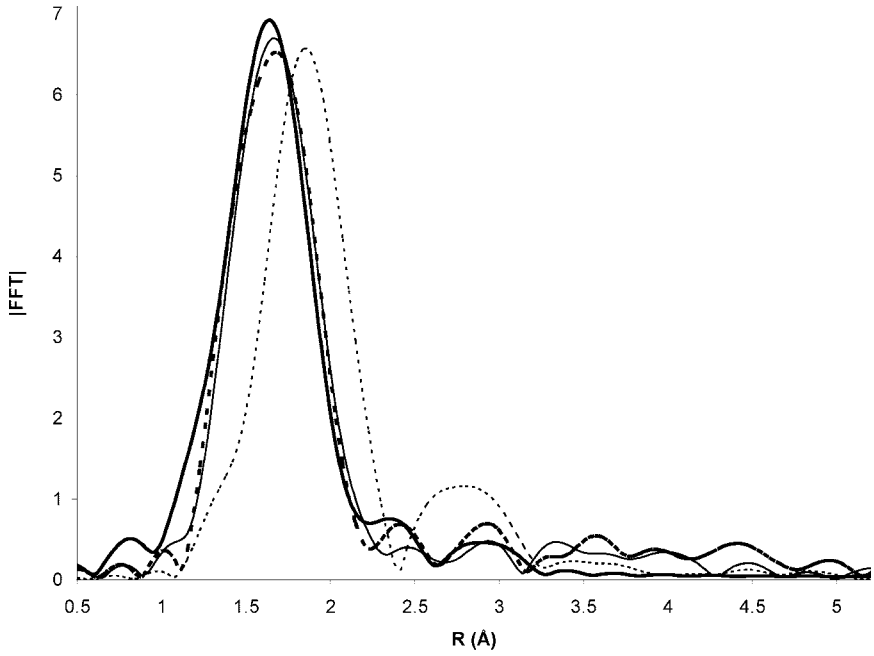

Figure 2. Rh K-edge FFT EXAFS spectra (not phase-corrected) of (---) Rh(cod); (—) Rh(cod)/SiO_2 (0.71 wt % Rh); (•••) Rh(cod)-Pd/SiO_2 (0.75–1.91 wt % Rh−Pd); and (▬) Rh(cod)-Pd/SiO_2 (0.75–1.91 wt % Rh−Pd) after exposure to air.

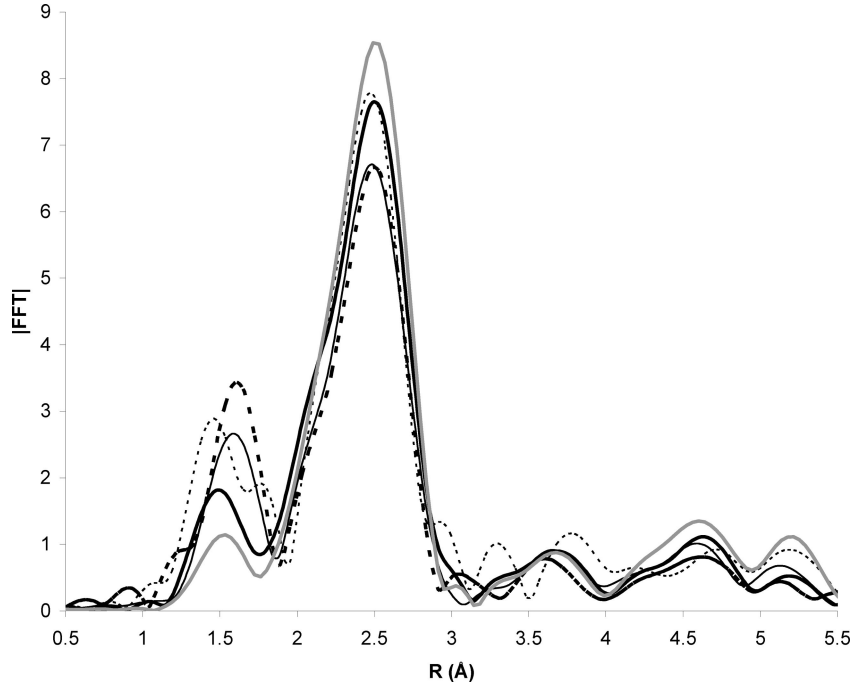

Figure 3. Pd K-edge FFT EXAFS spectra (not phase-corrected) of (—) Pd/SiO_2 (1.93 wt % Pd); (•••) Pd/SiO_2 (1.93 wt % Pd) after exposure to oxygen; (▬) Pd/SiO_2 (1.93 wt % Pd) after exposure to oxygen and treatment with CH_2Cl_2; (gray —) Rh(cod)-Pd/SiO_2 (0.75–1.91 wt % Rh−Pd); and (---) Rh(cod)-Pd/SiO_2 (0.75–1.91 wt % Rh−Pd) after exposure to air.

contribution from surface atoms or other adjacent species was detected for Rh(cod)/SiO_2 and Rh(cod)-Pd/SiO_2.

The Pd K-edge spectrum of Rh(cod)-Pd/SiO_2 (0.75–1.91 wt % Rh−Pd) showed a shell structure that is characteristic of *fcc* palladium metal particles, with a Pd−Pd nearest neighbors value (N_{Pd-Pd}) of 7.9 (Pd−Pd distance of 2.723 Å; Table 2, entry 4), while the peak trend for the next shells indicated the formation of small metal particles dispersed on the support with a small contribution from the surface oxygen atoms ($N_{Pd-O} = 1.2$). As the palladium foil has a *fcc* crystal frame with 12 nearest neighbors at 2.75 Å, on the assumption of particle growth with the same packing and cubooctahedric geometry, a mean diameter of ca. 18 Å was estimated for the palladium particles in Rh(cod)-Pd/SiO_2 (0.75–1.91 wt % Rh−Pd). This value is slightly larger than that measured before anchoring Rh(cod) ($N_{Pd-Pd} = 6$, corresponding to ca. 15 Å), which suggests that the impregnation procedure modifies somewhat the dispersion of the preformed palladium particles (Table 2, entry 1). The same behavior at the Pd K-edge was observed for Pd/SiO_2 (1.93 wt % Pd) after exposure to oxygen (Table 2, entry 2) followed by treatment with anhydrous CH_2Cl_2 (Table 2, entry 3), the solvent used to anchor Rh(cod), which confirms that a palladium particle

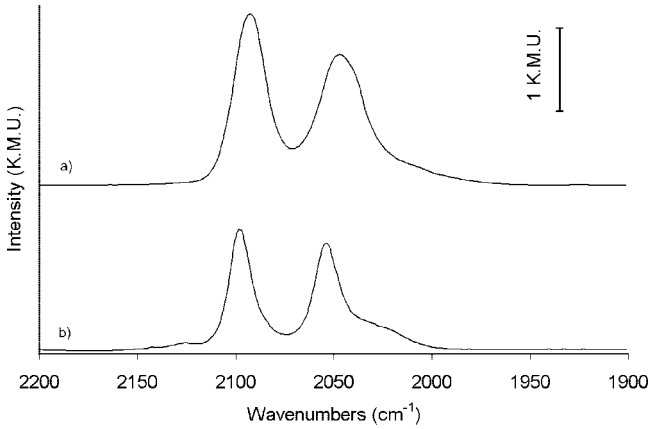

Figure 4. DRIFTS spectra of (a) Rh(cod) and (b) Rh(cod)/SiO_2 (0.71 wt % Rh) after CO exposure (1 bar flow, room temperature, 15 min) and purging in He flow.

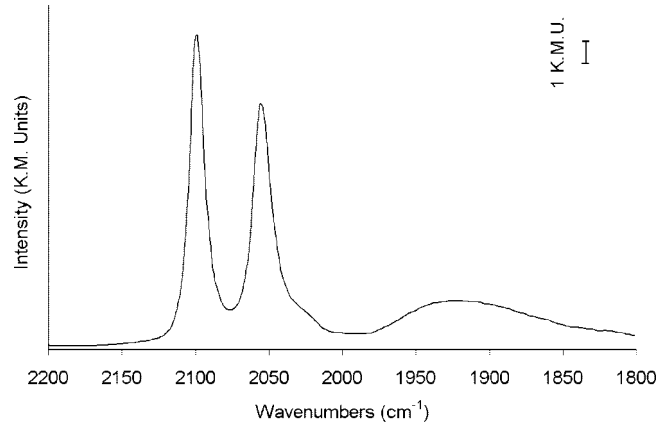

Figure 5. DRIFTS spectrum of Rh(cod)-Pd/SiO_2 (0.75–1.91 wt % Rh−Pd) after CO exposure (1 bar flow, room temperature, 15 min) and purging in He flow.

Scheme 4

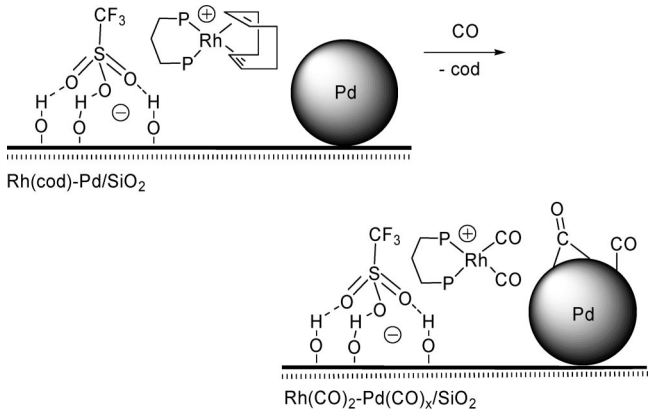

enlargement takes place irrespective of the presence of rhodium in the palladium surroundings. As reported in Table 2, all samples showed the presence of oxygen atoms at a bonding distance to palladium atoms. These oxygen atoms generally belong to the silanols of silica, but a palladium oxide contribution is present in just-impregnated Rh(cod)-Pd/SiO_2 (see Experimental Section) as well as in the samples exposed to air/oxygen.

DRIFTS Spectra of Carbonylated Rhodium Complexes and Silica-Supported Catalyst Precursors. Due to the absence of functional groups readily identifiable by IR spectroscopy, CO was used as a probe molecule to get structural and chemical information on the supported compounds by DRIFTS.

Solid Rh(cod), diluted with anhydrous KBr powder, was reacted with CO (1 bar flow) at room temperature for 15 min to yield a species with an IR spectrum containing two intense bands located at 2093 and 2047 cm^{-1} (Figure 4a), which were readily ascribed to the symmetric and antisymmetric stretch vibrations of the cis-dicarbonyl complex $Rh(CO)_2$.[18] The supported form of the latter complex, Rh(CO)$_2$/SiO_2, was obtained by carbonylation of Rh(cod)/SiO_2 (0.71 wt % Rh), as shown by the IR spectrum of the resulting product, containing two analogous bands at 2098 and 2054 cm^{-1} (Figure 4b).

The replacement of the cod ligand in Rh(cod)/SiO_2 by two CO molecules also modified the C−H stretching region, allowing us to determine some absorptions bands of the C−H vibrations of cod (3014, 3067 cm^{-1}). The small difference in wavenumbers and line width between $Rh(CO)_2$ and Rh(CO)$_2$/SiO_2 can be accounted for by the different physical status of the two compounds. The former is a classical cationic metal complex where cations and anions are packed in a crystal lattice. In contrast, in Rh(CO)$_2$/SiO_2 the triflate anions are anchored to the silica surface by H-bonding and the complex cations are kept close to the triflate-functionalized silica surface exclusively by electrostatic interaction, which allows for a relatively high degree of mobility and flexibility. Consistently, the IR spectrum of $Rh(CO)_2$ in a solvent containing hydroxyl groups such as ethylene glycol showed ν(CO) bands exactly at 2098 and 2054 cm^{-1}.[23] It is noteworthy that two IR bands in the range from 2038 to 2096 cm^{-1} are typical for a number of surface-constrained Rh^I complexes, whereas Rh^0 particles generally exhibit a single band from 2040 to 2066.[24] The bands observed for Rh(CO)$_2$/SiO_2 are therefore in line with the literature data.

Upon carbonylation, Rh(cod)-Pd/SiO_2 (0.75–1.91 wt % Rh−Pd) was converted to Rh(CO)$_2$-Pd(CO)$_x$/SiO_2 (Scheme 4) containing electrostatically tethered $[Rh(CO)_2(dppp)]^+$ cations, as shown by the appearance of IR bands at 2099 and 2055 cm^{-1} (Figure 5). In addition, to these bands, the spectrum also contained a band at 1925 cm^{-1}, which can be ascribed to bridging CO groups adsorbed on palladium metal particles.[25] The band due to linear CO on palladium nanoparticles, usually located at 2100 cm^{-1}, was not detected, as it falls in the same region of the more intense symmetric ν(Rh−CO) absorption.

EXAFS Studies of Rh(cod)-Pd/SiO_2 Exposed to Air. The effects caused by the exposure of Rh(cod)-Pd/SiO_2 to air, hence to O_2 and moisture, has been checked in an attempt to obtain information on the stability of this catalytic system as well as detect possible structural changes caused by the use in catalysis of recycled catalysts recovered without the protection of an inert gas (vide infra).

The Fourier spectra at the Rh K-edge of Rh(cod)-Pd/SiO_2 (0.75–1.91 wt % Rh−Pd) before and after being exposed to air overnight at room temperature are reported in Figure 2 (Table 1, entries 4 and 5). No relevant modification of the rhodium coordination sphere apparently occurred, which demonstrates the excellent stability of the electrostatically immobilized $[Rh(cod)(dppp)]^+$ complex cation.

EXAFS Studies of the Hydrogenation Products of Rh(cod)/

(23) Lucenti, E.; Roberto, D.; Roveda, C.; Ugo, R.; Cariati, E. *J. Cluster Sci.* **2001**, *12*, 113.

(24) Stanger, K. J.; Tang, Y.; Anderegg, J.; Angelici, R. J. *J. Mol. Catal. A: Chem* **2003**, *202*, 147, and references therein.

(25) Liotta, L. F.; Martin, G. A.; Deganello, G. *J. Catal.* **1996**, *164*, 322, and references therein.

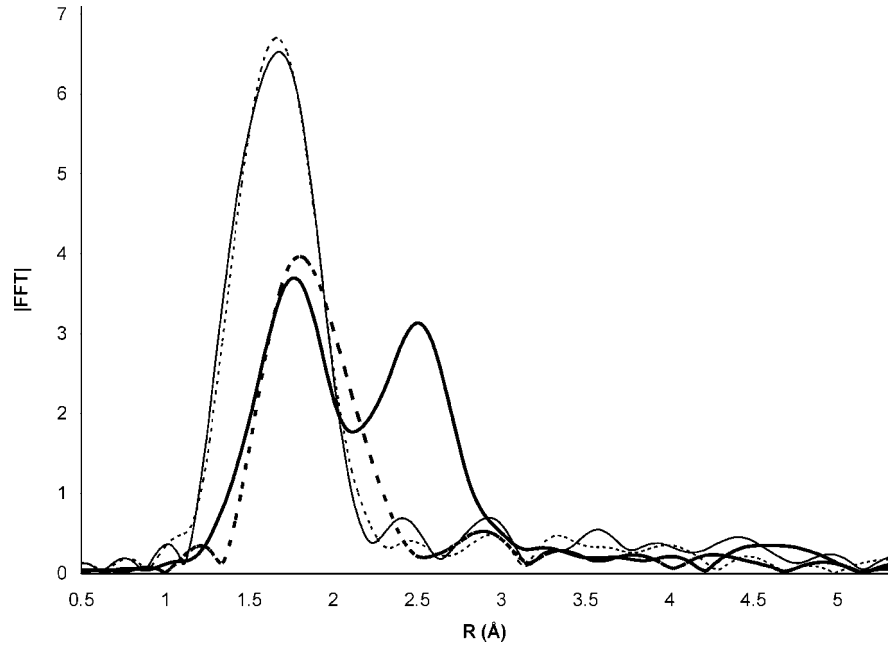

Figure 6. Rh K-edge FFT EXAFS spectra (not phase-corrected) of (•••) Rh(cod)/SiO_2 (0.71 wt % Rh); (---) Rh(cod)/SiO_2 (0.71 wt % Rh) after in situ reduction with H_2 flow at 120 °C; (—) Rh(cod)-Pd/SiO_2 (0.75–1.91 wt % Rh−Pd); and (−) Rh(cod)-Pd/SiO_2 (0.75–1.91 wt % Rh−Pd) after in situ reduction with H_2 flow at 120 °C.

Scheme 5

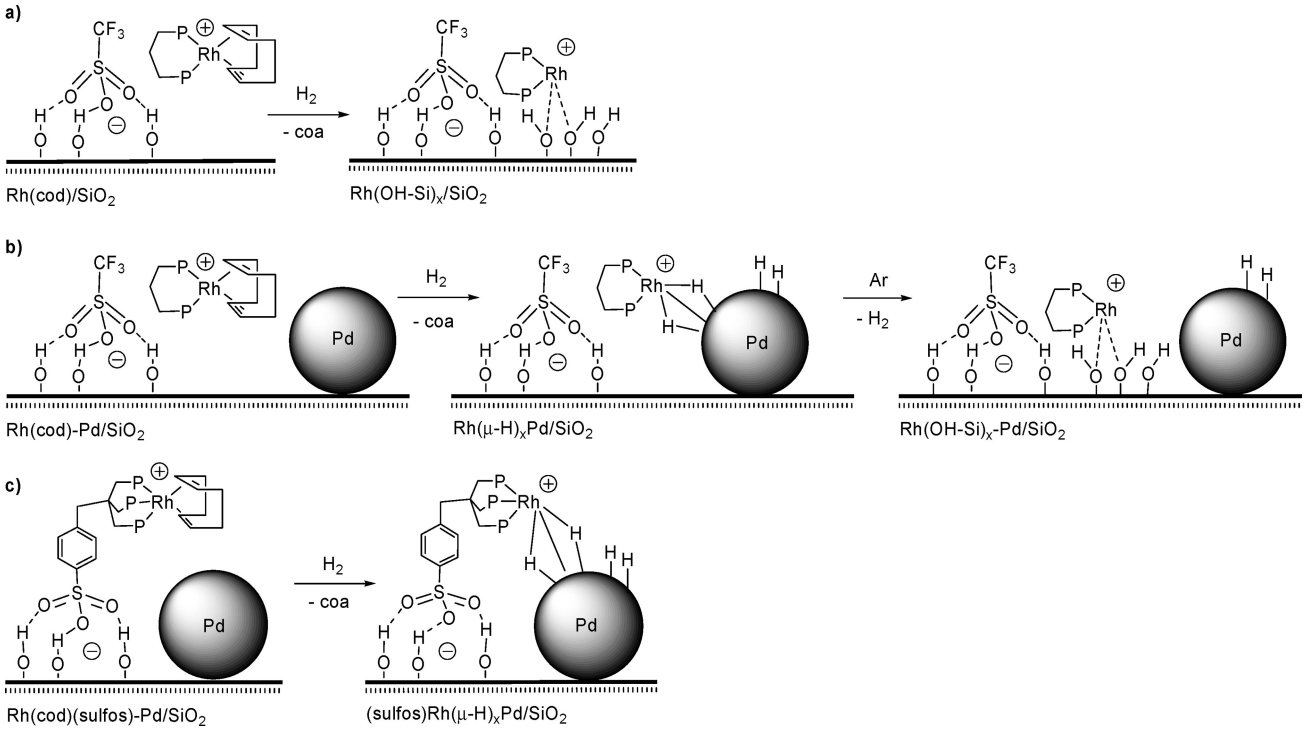

SiO_2 and Rh(cod)-Pd/SiO_2. Upon in situ treatment with H_2 at 120 °C (Figure 6; Table 1, entry 3), the cod ligand was removed from Rh(cod)/SiO_2 (0.71 wt % Rh) as coa (temperature-programmed reductive decomposition/quadrupole mass spectroscopy (TPRD/QMS) evidence). The EXAFS analysis of this sample showed each rhodium atom to be surrounded by two phosphorus atoms with Rh−P distances almost identical to those in Rh(cod) and by ca. three oxygen atoms at a distance of 2.330 Å, presumably from surface silanols interacting with the metal center (Scheme 5a). No further contribution was visible in the coordination shell of rhodium. This result, however, does not exclude the presence of hydride/dihydrogen ligands that cannot be detected by EXAFS.[17,26]

The EXAFS spectrum at the Rh K-edge of Rh(cod)-Pd/SiO_2 (0.75–1.91 wt % Rh−Pd) after in situ reduction with H_2 at 120 °C (coa formation) showed two distinct peaks (Figure 6; Table 1, entry 6). In addition to two phosphorus atoms with Rh−P distances a little longer than those in the precursor, a relevant contribution from a palladium shell was actually detected ($N_{Rh-Pd} = 3.4$). In principle, it is not possible to discriminate palladium from rhodium as photoelectron scatterer, but the attribution of the Rh-metal shell to palladium neighbors was

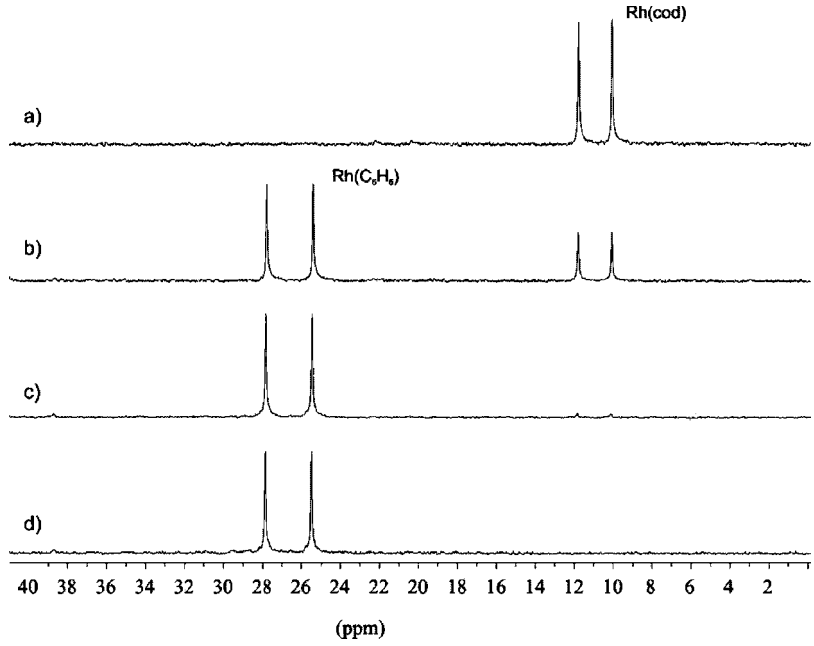

Figure 7. Variable–temperature $^{31}P\{^1H\}$ HPNMR study (THF-d_8, 81.01 MHz) of the hydrogenation reaction of Rh(cod) in the presence of 10-fold excess of C_6H_6: (a) under nitrogen at room temperature; (b) under H_2 (30 bar) after 5 min at room temperature; (c) after 30 min at room temperature; (d) at 40 °C.

unambiguously supported by the evidence that Rh(cod)/SiO_2 did not exhibit any Rh−Rh contribution even upon treatment with H_2 up to 300 °C. The Rh−Pd distance of 2.741 Å, only slightly longer than that reported for a Rh−Pd alloy (2.72 Å), and the number of Rh−Pd nearest neighbors of 3.4 (lower than the corresponding Pd−Pd value at the Pd K-edge in Rh(cod)-Pd/SiO_2; Table 2, entry 4) point to rhodium and palladium atoms in close proximity but not alloyed. Besides leading to the conversion of cod to coa, H_2 would react with the 12e$^-$ fragment $[Rh(dppp)]^+$, formed upon the last hydride-alkyl reductive migration, to give $[Rh(H)_x(H_2)_y(dppp)]^+$ species containing either classical or nonclassical hydride ligands. In turn, the palladium particles will react with H_2 to form surface Pd−H species. It is therefore likely that the observed Rh−Pd vicinity involves the formation of hydride-bridged Rh(μ-H)$_x$Pd species, featured by a metal−metal bond (Scheme 5b), as previously reported for the hydrogenation of Rh(cod)(sulfos)-Pd/SiO_2 (Scheme 5c).[2]

Noticeably, the Rh−Pd bond was observed by EXAFS only upon in situ hydrogenation of Rh(cod)-Pd/SiO_2 and maintaining the sample under a H_2 atmosphere during the spectral acquisition. Even very fast transfer of the product obtained by ex situ hydrogenation of Rh(cod)-Pd/SiO_2 to the EXAFS cell led to the disappearance of the hydride-mediated rhodium−palladium moiety and the $[Rh(dppp)]^+$ fragments were stabilized by interacting with the surface OH groups (Scheme 5b), as occurs when the cod ligand in Rh(cod)/SiO_2 is hydrogenated to coa (Scheme 5a).

The low propensity of dppp to form stable rhodium hydride complexes is witnessed by the lack of such complexes in the relevant literature.[17,26] Therefore, we were not surprised to find that the in situ homogeneous reaction of Rh(cod) with H_2 (30 bar) in THF-d_8 gave coa and several unidentified products, among which, only one hydride compound in trace amount (vide infra).

Homogeneous Modeling Studies. Hydrogenation Reaction of Rh(cod). The independent reaction of Rh(cod) with H_2 was studied by ^1H and $^{31}P\{^1H\}$ HPNMR spectroscopy in THF-d_8 in a 10 mm sapphire tube pressurized with 30 bar of H_2. The NMR analysis showed the complete disappearance of the starting complex already after 30 min at room temperature with formation of coa. Several Rh-dppp species were formed, among which there was the bis-solvento complex $[Rh(solv)_2(dppp)]OTf$ (solv = THF, adventitious water; $^{31}P\{^1H\}$ NMR: δ 40.1 (d, J_{RhP} = 190.5 Hz)) in 35% yield.[17] Notably, only a trace amount of a hydride compound, featured by a ^1H NMR multiplet at δ –22.02, was formed. The behavior of Rh(cod) under hydrogenation conditions reflects the elusive nature of polyhydride rhodium complexes with chelating diphosphine ligands.[17,26] These compounds, which may also exhibit nonclassical dihydrogen (η^2-H_2) structure,[29] have a great tendency to lose H_2 upon reaction with mild nucleophiles.[26]

Hydrogenation Reaction of Rh(cod) with H_2 in the Presence of Benzene. The reaction of Rh(cod) with H_2 was performed in THF-d_8 also in the presence of benzene and followed in situ by ^1H and $^{31}P\{^1H\}$ HPNMR spectroscopy. Figure 7 shows the $^{31}P\{^1H\}$ NMR spectra obtained at different temperatures and acquisition times. At room temperature, Rh(cod) was completely transformed into Rh(C_6H_6) within 30 min. The latter compound was the only NMR-visible species at 40 °C for 1 h. The ^1H NMR spectra showed also the formation of coa, while no trace of benzene-hydrogenation products was detected by GC/MS. Significant decomposition of Rh(C_6H_6)

(26) Douglas, T. M.; Brayshaw, S. K.; Dallanegra, R.; Kociok-Köhn, G.; Macgregor, S. A.; Moxham, G. L.; Weller, A. S.; Wondimagegn, T.; Vadivelu, P. *Chem.−Eur. J.* **2008**, *14*, 1004.

(27) (a) Buisman, G. J. H.; van der Veen, L. A.; Kamer, P. C. J.; van Leeuwen, P. W. N. M. *Organometallics* **1997**, *16*, 5681. (b) Buisman, G. J. H.; Vos, E. J.; Kamer, P. C. J.; van Leeuwen, P. W. N. M. *Dalton Trans.* **1995**, 409. (c) Kiss, G.; Horváth, I. *Organometallics* **1991**, *10*, 3798. (d) Bianchini, C.; Meli, A.; Peruzzini, M.; Vizza, F.; Frediani, P.; Ramirez, J. A. *Organometallics* **1990**, *9*, 226.

(28) Chen, C. S.; Lin, J. H.; Chen, H. W. *Appl. Catal., A* **2006**, *298*, 161.

(29) Bakhmutov, V. I.; Bianchini, C.; Peruzzini, M.; Vizza, F.; Vorontsov, E. V. *Inorg. Chem.* **2000**, *38*, 1655.

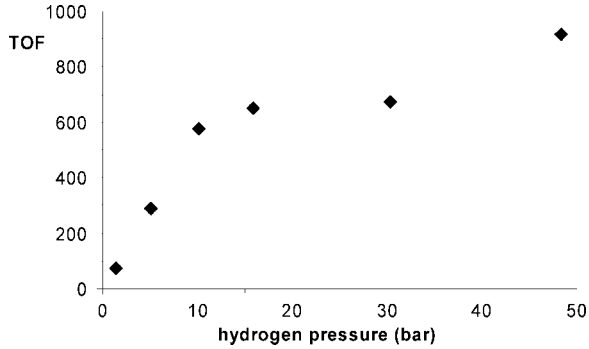

Figure 8. Hydrogenation reactions of benzene catalyzed by Rh(cod)-Pd/SiO_2 (Table 4, entries 1–6). Dependence of the rate on H_2 pressure.

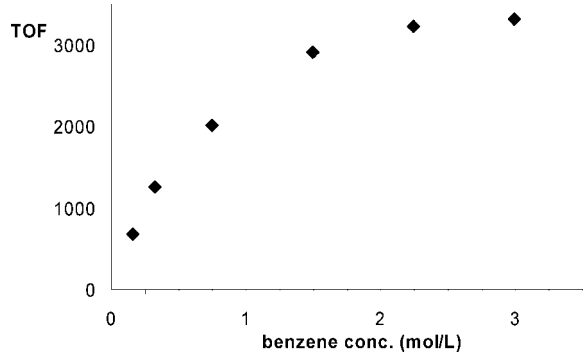

Figure 9. Hydrogenation reactions of benzene catalyzed by Rh(cod)-Pd/SiO_2 (Table 4, entries 5, 7–11). Dependence of the rate on benzene concentration.

occurred only above 80 °C, to give several unidentified products, among which we noticed a hydride compound in a trace amount (^{1}H NMR multiplet at δ −22.71).

Synthesis of Rh(C_6H_6). A solution of Rh(cod) in 40 mL of a 3:1 (v/v) THF/benzene mixture was hydrogenated (30 bar H_2) in an autoclave at room temperature for 30 min with stirring. Evaporation of the reaction mixture under reduced pressure gave the benzene complex Rh(C_6H_6) as a yellow solid in analytically pure form. Unambiguous identification of the latter complex was achieved by NMR spectroscopy in CD_2Cl_2, also by comparison with the spectra of $[Rh(benzene)(diphos)]^+$ (diphos = 1,2-bis(diphenylphosphino)ethane).[30] Noteworthy, dissolving Rh(C_6H_6) in THF-d_8 or MeOH-d_4 under nitrogen generated bis-solvento complexes analogous to those described above, which reflects the great oxophilicity of the $[Rh(dppp)]^+$ fragment.[17]

Catalytic Hydrogenation of Benzene by Rh(cod)-Pd/SiO_2. The hydrogenation reactions were generally carried out with 0.43 mL of benzene under 30 bar H_2 in *n*-pentane (complement to 30 mL total volume) at 40 °C for 2 h. Under these experimental conditions, Rh(cod)/SiO_2 did not catalyze the hydrogenation of benzene (Table 3, entry 7), while Pd/SiO_2 yielded cyclohexane with a TOF of 72 μmol of product h^{-1} (Table 3, entry 1). A much higher TOF was obtained using the hybrid catalyst Rh(cod)-Pd/SiO_2 even at very low rhodium content (Table 3, entries 2–5). The same TOF as in entry 1 was obtained by using a mechanical mixture of Pd/SiO_2 (47 mg, 1.93 wt % Pd) and Rh(cod)/SiO_2 (47 mg, 0.65 wt % Rh), which confirmed the occurrence of enhanced activity only when the Rh^I single sites and the palladium particles are concomitantly anchored to the support.

(30) Landis, C. R.; Halpern, J. *Organometallics* **1983**, *2*, 840.

Scheme 6

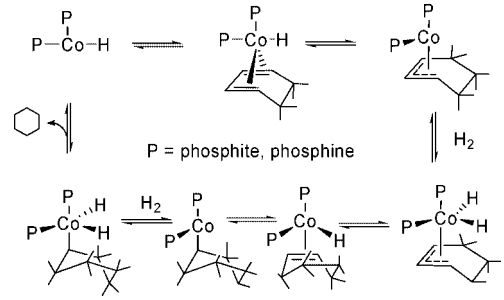

Chart 1

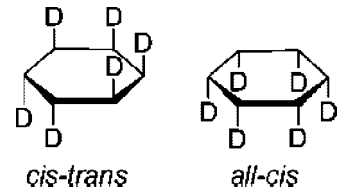

To get information on the mechanism of benzene hydrogenation to cyclohexane by Rh(cod)-Pd/SiO_2 catalysis, especially as regards the synergic action of the rhodium single sites and the palladium nanoparticles, we decided to perform a study where H_2 pressure, substrate concentration, rhodium to palladium ratio, and catalyst amount were systematically varied (Tables 3 and 4). Partial benzene hydrogenation products were not detected by GC/MS at any stage of the reactions. The catalytic activity, in terms of dependence of benzene conversion on H_2 pressure, benzene concentration, and catalyst amount, was evaluated by using two different Rh(cod)-Pd/SiO_2 catalyst precursors (1.00–1.59 wt % Rh−Pd and 0.65–1.58 wt % Rh−Pd). The dependence of substrate conversion on the rhodium content in the catalyst precursor was evaluated with samples of Rh(cod)-Pd/SiO_2 containing from 0.07 to 1.07 wt % Rh (1.87–1.91 wt % Pd).

From a perusal of the TOFs obtained by varying the amount of rhodium (Table 3, entries 2–5), one may readily infer that, in the interval of rhodium loading examined, the hydrogenation rate of benzene shows a little dependence on the amount of the tethered single site component (the TOF increases from 491 to 644 for a rhodium amount increasing from 0.07 to 1.07 wt %). On the other hand, rhodium contents significantly lower than 0.07 wt % in Rh(cod)-Pd/SiO_2 were not investigated because of the poor synthetic reproducibility and the unreliable elemental analysis.

On the assumption of palladium nanoparticles with a mean diameter of ca. 18 Å (Table 2), there would be ca. 40 palladium atoms per nanoparticle with a percentage of superficial atoms between 50% and 80%.[2,31] Therefore, in a sample of Rh(cod)-Pd/SiO_2 containing 0.07 wt % Rh and 1.87 wt % Pd, every palladium nanoparticle would have a maximum of ca. 3 potentially interacting $[Rh(dppp)]^+$ fragments. This number would increase to 12 already in Rh(cod)-Pd/SiO_2 with 0.27 wt % Rh and to 50 in Rh(cod)-Pd/SiO_2 with 1.07 wt % Rh. At the latter rhodium loadings, the steric and electrical (cation–cation repulsion) crowding may be excessive for 18 Å metal particles.

(31) (a) Sergeev G. B. *Nanochemistry*; Elsevier: Amsterdam, 2006. (b) Beck, A.; Horváth A.; Sárkány, A.; Guczi. L. In *Nanotechnology in Catalysis*; Zhou, B., Hermans, S., Somorjai, G. A., Eds.; Springer: Berlin, 2004; Vol. 1, Chapter 5. (c) Haw, J. F.; Marcus, D. M. In *Nanotechnology in Catalysis*; Zhou, B., Hermans, S., Somorjai, G. A., Eds.; Springer: Berlin, 2004; Vol. 1, Chapter 13.

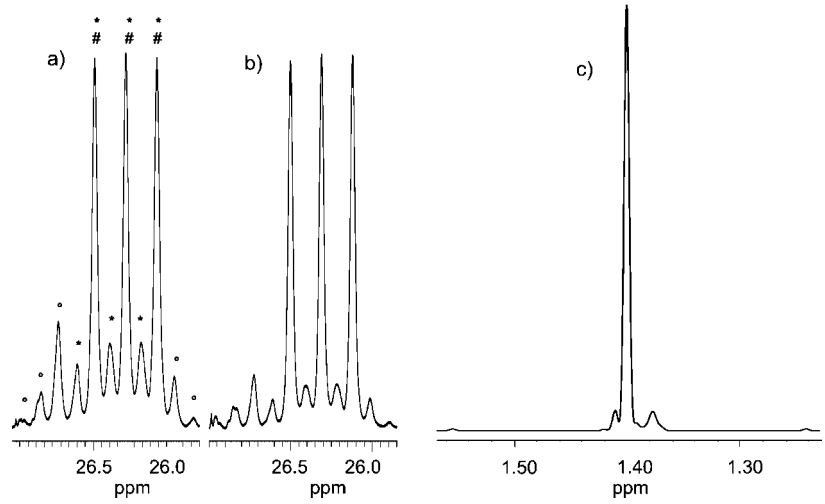

Figure 10. NMR spectra (21 °C, C_6H_6-d_6) in the cyclohexane region of the mixtures of products obtained by hydrogenation of C_6H_6-d_6 in the presence of Pd/SiO_2 (1.93 wt % Pd) ($^{13}C\{^1H\}$ NMR, 100.613 MHz, a) and Rh(cod)-Pd/SiO_2 (0.75–1.91 wt % Rh−Pd) ($^{13}C\{^1H\}$ NMR, 100.613 MHz, b; $^2H\{^1H\}$ NMR, 61.423 MHz, c). Representative resonances attributed to all-cis, cis–trans mixture, and disproportionation products are marked with #, *, and °, respectively.

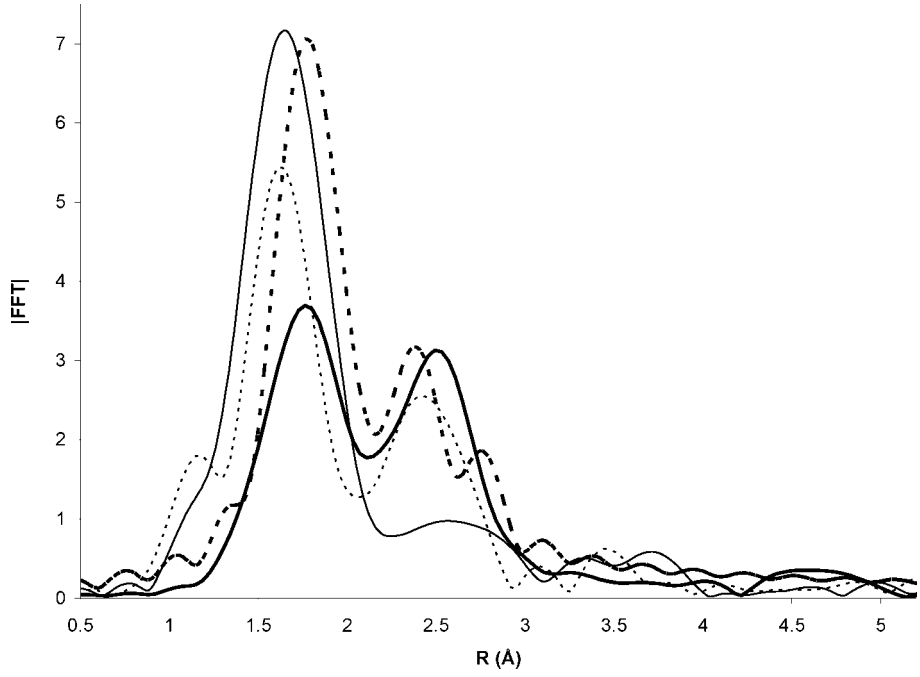

Figure 11. Rh K-edge FFT EXAFS spectra (not phase-corrected) of recovered catalysts derived from Rh(cod)-Pd/SiO_2 (0.75–1.91 wt % Rh−Pd): (•••) after a catalytic run to 33% benzene conversion (30 bar, 40 °C, 2 h); (—) after a catalytic run to 33% benzene conversion (30 bar, 40 °C, 2 h) and exposure to air; (---) after a catalytic run to 33% benzene conversion (30 bar, 40 °C, 2 h) and exposure to air followed by a second catalytic run to 68% benzene conversion (30 bar, 40 °C, 24 h). As a comparison (**—**) Rh(cod)-Pd/SiO_2 (0.75–1.91 wt % Rh−Pd) after in situ reduction with H_2 flow at 120 °C.

It is therefore likely that the majority of the $[Rh(dppp)]^+$ fragments will not have any chance to interact with the palladium particle. In this eventuality, the small dependence of the TOF on the rhodium amount in the catalyst might be simply due to a saturation effect, as only the rhodium single sites interacting with the palladium atoms are catalytically active for benzene hydrogenation (vide infra). In searching for further evidence supporting this concept, two Rh(cod)-Pd/SiO_2 samples with Rh loadings of 0.08 and 0.70 wt % were prepared using a Pd/SiO_2 support with a metal loading of 9.86 wt %. HRTEM and EXAFS analyses of the latter material showed a metal dispersion quite comparable to that of the analogous material used to synthesize the catalysts of entries 1–6 in Table 3.[2] The TOFs of benzene hydrogenation catalyzed by these new Rh(cod)-Pd/SiO_2 compounds were 841 for the sample containing 0.07 wt % Rh (entry 8) and 1241 for the sample with 0.70 wt % Rh (entry 9). While the increased Pd loading in the catalyst of entry 8, as compared to the catalyst of entry 2, can well account for the higher TOF (841 vs 491), the much higher TOF observed for the catalyst of entry 9, as compared to the catalyst of entry 4 (1241 vs 597), cannot be solely justified by the increased Pd loading. Again, a substantial role in enhancing the catalytic activity seems to be played by a more effective interaction between the rhodium single sites and the surface palladium atoms, whose number increases by increasing the palladium loading at constant metal dispersion. In other words,

Scheme 7

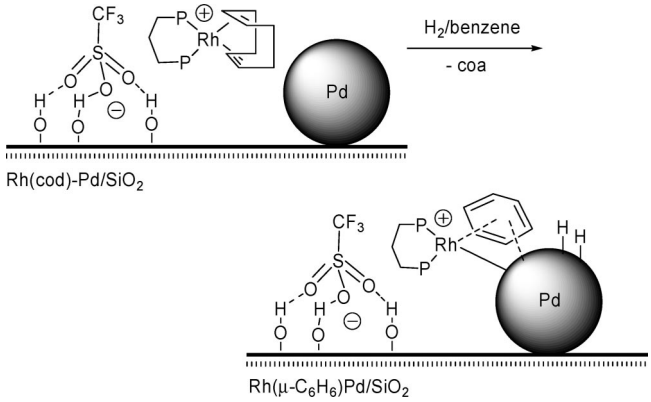

the $[Rh(dppp)]^+$ fragments which have no chance to interact with the palladium particles in the catalyst with 1.91–0.75 wt % Pd−Rh seem to be operative in the catalyst with 9.86–0.70 wt % Pd−Rh, thus leading to increased benzene conversion.

Although kinetically irrelevant, the study of the TOF dependence on the rhodium loading has confirmed that Rh^I single sites and not Rh^0 metal particles take part in the catalytic process. Indeed, the fact that the TOF does not increase by increasing the rhodium loading from 0.07 to 1.07 wt % rules out any role of Rh^0 metal particles in the hydrogenation of benzene (as shown also by the EXAFS studies on Rh(cod)-Pd/SiO_2 and Rh(cod)/SiO_2 upon treatment with H_2). In fact, were the formation of Rh^0 metal particles responsible for the hydrogenation of the substrate, then one would have observed an increase of the TOF by increasing the rhodium amount in the precursor.[24]

A plot of TOF vs H_2 pressure gave an almost a linear correlation for H_2 pressures lower than 10 bar, while a saturation effect apparently occurred at higher H_2 pressures, featured by a plateau of activity (Table 4; Figure 8).

The TOF tended to plateau also at substrate concentrations higher than 0.7 mol/L (Table 4; Figure 9), while an almost linear correlation was observed at lower catalyst amounts.

Finally, a linear correlation between TOF and catalyst amount was found keeping H_2 pressure (30 bar) and benzene concentration (0.161 M) constant (Table 4, entries 12–14).

The physical and chemical stability of the TCSM catalyst derived from Rh(cod)-Pd/SiO_2 against leaching from the support was proved by a series of recycling experiments reported in Table 5. In all cases, after the liquid phase was separated from the solid catalyst, the solvent was removed under vacuum and the residue was analyzed by both $^{31}P\{^1H\}$ NMR spectroscopy and ICP-AES. No trace of phosphorus was seen by NMR spectroscopy, while the amount of rhodium detected by ICP-AES was invariably <1 ppm. After performing a catalytic run with Rh(cod)-Pd/SiO_2 (0.73–1.50 wt % Rh−Pd) (Table 5, entry 1), the solvent was decanted under nitrogen in a drybox and the remaining solid was washed with *n*-pentane until no trace of benzene or cyclohexane was detected by GC/MS in the liquid phase; then the catalyst was reused for a second run (entry 2). This recycling procedure was repeated for a third run (entry 3). Finally, the catalyst recovered from the second recycle was exposed to air for 2 days at room temperature before being employed in a further reaction (entry 4). Consistent with a great stability of the TCSM catalyst, comparable TOFs were obtained in the first three reactions. When, however, the recycled catalyst was exposed to air prior to a further use, the TOF increased from 717 to 919 (entries 3 and 4). Evidence for a significant activity enhancement in benzene hydrogenation by air-treated silica-supported Pd nanoparticles has been reported by Guczi et al.[32] According to this author, the treatment in air at high temperature does not change the particle dimensions, whereas it contributes to restructure the particle surface as a consequence of impurities removal as well as the PdO/Pd transition in the subsequent hydrogen treatment. In the present case, a further complication might be provided by the presence of the tethered rhodium complex. In an attempt to rationalize the enhancing effect of air exposure, EXAFS analyses of recycled catalysts, prior and after exposure to air, have been carried out (vide infra).

Pd/SiO_2, Rh(cod)/SiO_2, and Rh(cod)-Pd/SiO_2 were also scrutinized as catalysts for the hydrogenation of either cyclohexa-1,3-diene or cyclohexene, which are possible intermediates along the reduction of benzene to cyclohexane. The results obtained are given in Table 6. From a perusal of the data relative to cyclohexa-1,3-diene hydrogenation (entries 1–3), one may readily realize that Rh(cod)/SiO_2 is more effective than Pd/SiO_2 and comparable to the hybrid system Rh(cod)-Pd/SiO_2. A comparison of the data (yields and TOFs) reported in Tables 3−6 also indicates that the rate-determining step in the hydrogenation of benzene to cyclohexane by Rh(cod)-Pd/SiO_2 is just the disruption of the substrate aromaticity upon addition of the first H_2 molecule. Even by taking into account the intrinsic ability of palladium nanoparticles to disproportionate cyclohexa-1,3-diene into benzene and cyclohexene (entry 4),[2] the much larger amount of residual cyclohexene in the reaction catalyzed by Pd/SiO_2 (entry 1), as compared to the reaction promoted by Rh(cod)/SiO_2 (entry 2), is a clear indication that the single-site catalyst is more efficient also for the reduction of *adsorbed* cyclohexene. This result, corroborated by the deuterium labeling study reported below, suggests that the hydrogenation of cyclohexa-1,3-diene to cyclohexane by Rh(cod)/SiO_2 proceeds via an associative mechanism similar to that reported by Muetterties for the Co^I catalyst $[CoH(PR_3)_2]$ (PR_3 = phosphite, phosphine) (Scheme 6).[33]

Only when cyclohexa-1,3-diene was replaced by cyclohexene as initial substrate (entries 5–7) was Pd/SiO_2 more active (entry 5) than Rh(cod)/SiO_2 (entry 6), which reflects the troublesome coordination of cyclic olefins to sterically hindered transition metal fragments such as the $[Rh(dppp)]^+$ ones.[34]

Benzene Hydrogenation Regiochemistry. The regiochemistry of C_6H_6-d_6 hydrogenation in the presence of either Pd/SiO_2 (1.93 wt % Pd) or Rh(cod)-Pd/SiO_2 (0.75–1.91 wt % Rh−Pd) was examined by $^{13}C\{^1H\}$ and $^2H\{^1H\}$ NMR spectroscopy. Previous reports in the literature for heterogenized single-site catalysts, specifically organoactinides and organozirconium complexes, showed the formation of mixtures of all-cis and cis–trans isotopomers, with a prevalence of the latter.[35] In contrast, the homogeneous hydrogenation of benzene catalyzed by $(\eta^3\text{-}C_3H_5)Co(PR_3)_3$ (PR_3 = phosphite, phosphine) has been found to give exclusively the all-cis product.[36]

(32) Horváth, A.; Beck, A.; Sárkány, A.; Koppány, Zs.; Szucs, A.; Dékány, I.; Horváth, Z. E.; Guczi, L. *Solid State Ionics* **2001**, *141–142*, 147.

(33) (a) Bleeke, J. R.; Muetterties, E. L. *J. Am. Chem. Soc.* **1981**, *103*, 556. (b) Stuhl, L. S.; Rakowski Du Bois, M. C.; Hirsekorn, F. J.; Bleeke, J. R.; Stevens, A. E.; Muetterties, E. L. *J. Am. Chem. Soc.* **1978**, *100*, 2405. (c) Rakowski, M. C.; Hirsekorn, F. J.; Stuhl, L. S.; Muetterties, E. L. *Inorg. Chem.* **1976**, *15*, 2379. (d) Muetterties, E. L.; Hirsekorn, F. J. *J. Am. Chem. Soc.* **1974**, *96*, 4063. (e) Muetterties, E. L.; Hirsekorn, F. J. *J. Am. Chem. Soc.* **1974**, *96*, 7920.

(34) Schrock, R. R.; Osborn, J. A. *J. Am. Chem. Soc.* **1976**, *98*, 4450.

(35) (a) Ahn, H.; Nicholas, C. P.; Marks, T. J. *Organometallics* **2002**, *21*, 1788. (b) Eisen, M. S.; Marks, T. J. *J. Am. Chem. Soc.* **1992**, *114*, 10358.

(36) Muetterties, E. L.; Rakowski, M. C.; Hirsekorn, F. J.; Larson, W. D.; Bauss, V. J.; Anet, F. A. L. *J. Am. Chem. Soc.* **1975**, *97*, 1266.

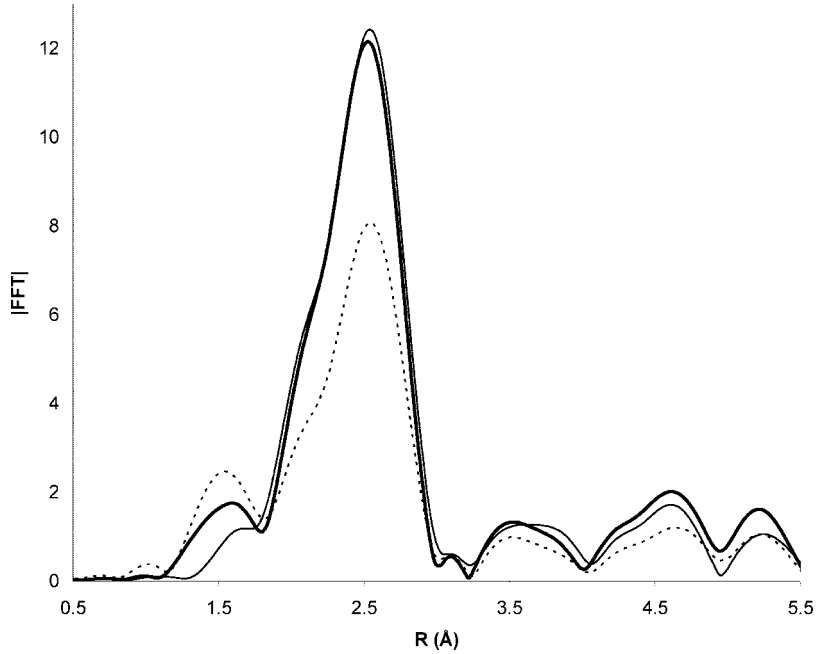

Figure 12. Pd K-edge FFT EXAFS spectra (not phase-corrected) of (—) Rh(cod)-Pd/SiO_2; (···) Rh(cod)-Pd/SiO_2 after a catalytic run to 33% benzene conversion (30 bar, 40 °C, 2 h) and exposure to air; and (−) Rh(cod)-Pd/SiO_2 after a catalytic run to 33% benzene conversion (30 bar, 40 °C, 2 h) and exposure to air followed by a second catalytic run to 68% benzene conversion (30 bar, 40 °C, 24 h).

Scheme 8

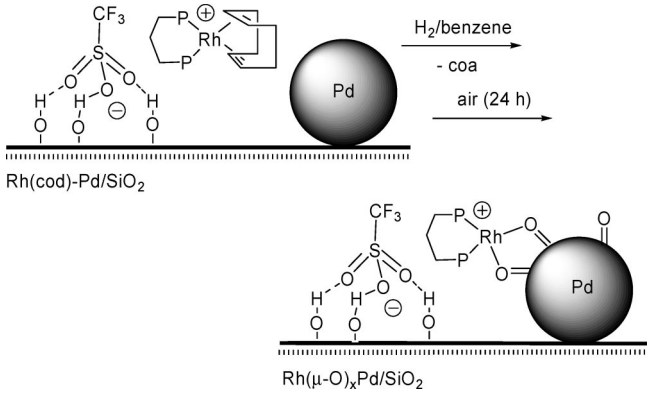

The $^{13}C\{^1H\}$ NMR spectrum of the product obtained with Pd/SiO_2 (Figure 10a) showed the formation of several regioisomers $C_6H_{6+x}D_{6-x}$, consistent with the hydrogenation of benzene to cyclohexane and with the disproportionation of cyclohexa-1,3-diene to benzene and cyclohexene.[2a,35b]

This means that also C−H/C-D exchange can be achieved. The major product was the $C_6H_6D_6$ cis–trans/all-cis isotopomer mixture (Chart 1).

The $^{13}C\{^1H\}$ and $^2H\{^1H\}$ NMR spectra of the product obtained with Rh(cod)-Pd/SiO_2 showed a much higher proportion of the all-cis isotopomer (Figure 10, b and c, respectively). The still complex isotopomer distribution obtained with Rh(cod)-Pd/SiO_2 can be accounted for by the concomitant presence of palladium, yet the largely increased proportion of the all-cis product suggests a prevalent role of the rhodium single sites along the hydrogenation path down to cyclohexane, once benzene is reduced to cyclohexa-1,3-diene with the mandatory assistance of the palladium nanoparticles (vide supra).

EXAFS and DRIFTS Studies of Recovered Catalysts. The catalytic materials recovered after quenching selected benzene hydrogenation reactions were studied by EXAFS and DRIFTS. The first EXAFS analysis was carried out on a product obtained after 33% conversion of benzene to cyclohexane in the presence of Rh(cod)-Pd/SiO_2 in *n*-pentane. The sample was transferred from the autoclave into the EXAFS sample holder under argon in a drybox. Under these conditions, a Rh−Pd shell was clearly evident at the same distance (Figure 11; Table 1, entry 7) as in the sample hydrogenated under solid–gas conditions (Table 1, entry 6), which means that a surface species with rhodium single sites and palladium particles bonded to each other is formed upon quenching the reaction. Notably, this species exhibits a significant C contribution, up to six neighbors, which suggests that benzene or some of the possible hydrogenation intermediates (cyclohexene, cyclohexa-1,3-diene) are coordinated to the rhodium sites in the quenched catalyst.

The former hypothesis, i.e., the coordination of benzene by the Rh−Pd moiety, is much more likely than any other in view of the fact that the η^6-C_6H_6 adduct Rh(C_6H_6) is an isolable product (vide supra). Scheme 7 shows a possible structure for the product recovered after quenching the benzene hydrogenation reaction at 33% conversion.

The benzene substrate in Scheme 7 has been drawn as a bridging ligand between the rhodium single site and surface palladium atoms (dual activation). Even though quite speculative, this representation has the merit of being consistent with both the EXAFS data and the reactivity of Rh(cod) in homogeneous phase and of Rh(cod)/SiO_2 in heterogeneous phase. Indeed, neither catalyst is able to hydrogenate benzene even under drastic experimental conditions, which points unambiguously to a key role of the palladium nanoparticles in the activation of benzene. Further support for this hypothesis was provided by the use of either Rh(C_6H_6)/SiO_2 or Rh(C_6H_6)-Pd/SiO_2 as catalyst precursor. The former species was completely inactive, whereas the latter was even more active than Rh(cod)-Pd/SiO_2, which may be due to a catalyst precursor already bearing the substrate (Table 3, entry 6 vs Table 3, entries 3–5 and Table 4 entries 5, 13).

The surprising increase in productivity observed for catalysts recovered in the air (Table 5, entry 4 vs entry 3) prompted us to study by EXAFS the effect of air exposure on a recycled

Scheme 9

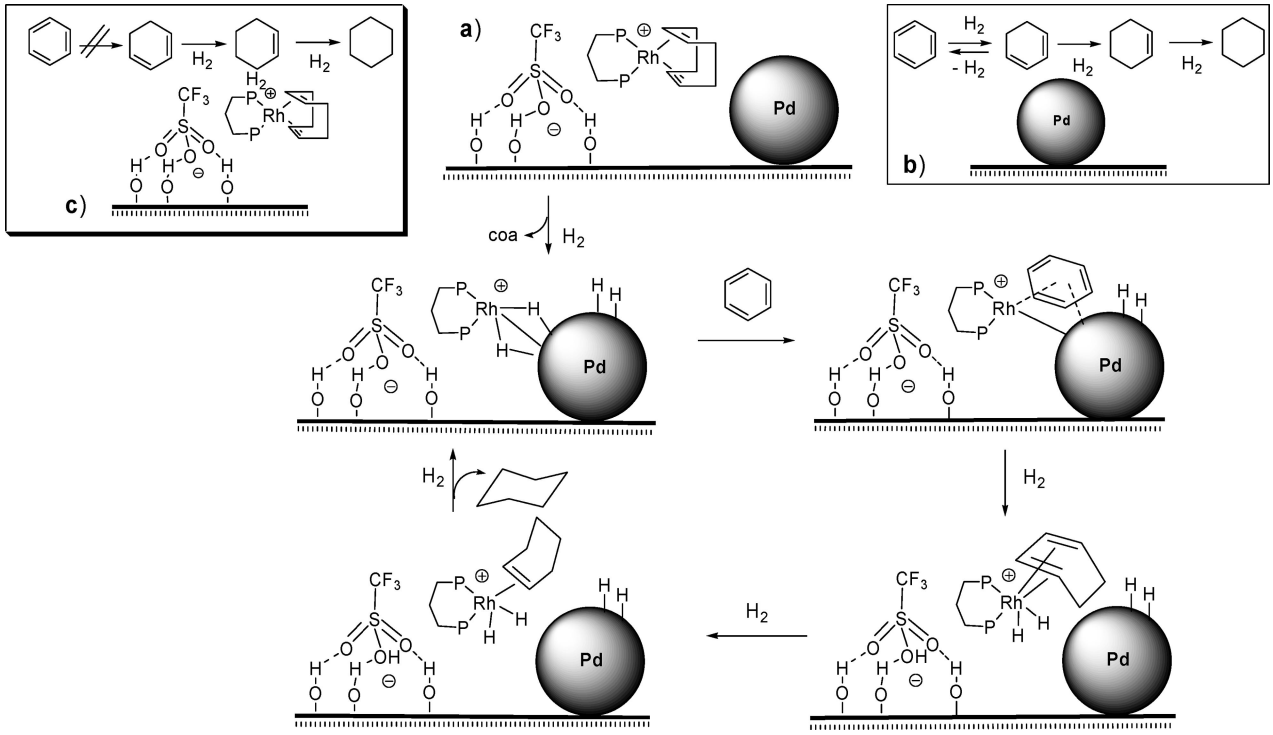

Scheme 10

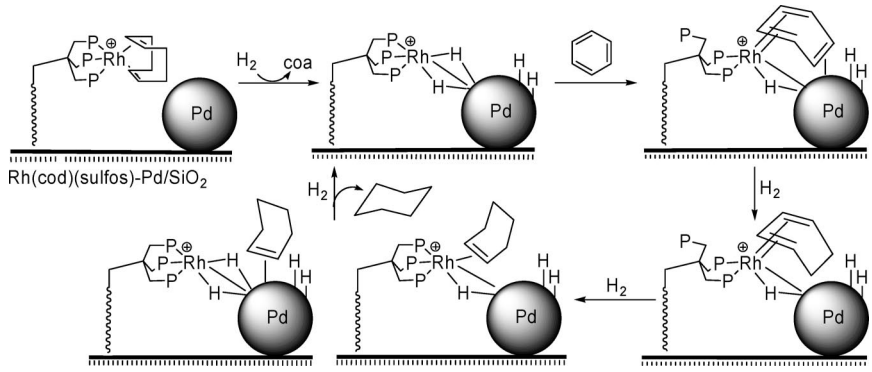

catalyst at 33% conversion (Figure 11; Table 1 entry 8). The two phosphorus atoms of the dppp ligand were still in the first shell, but a contribution of 1.6 palladium atoms appeared at a distance corresponding to the second neighboring shell of rhodium. Moreover, an average number of two oxygen atoms was detected at a rather short bonding distance (1.980 vs 2.330 Å of the Rh−silanol interaction), consistent with the formation of a Rh−O interaction (Table 1, entries 3 and 8). These findings suggest that the $[Rh(dppp)]^+$ fragments interact with the thin oxide layer over the palladium nanoparticles, formed upon exposure to air, so as to originate a Rh−O−Pd array. Within this context, it is worth restating that the binding affinity of $[Rh(dppp)]^+$ moieties to oxygen atoms has been unambiguously proven in both the solid state (see Scheme 5) and solution (see homogeneous modeling studies).[17] In agreement with the oxidation of a fraction of surface palladium atoms, the EXAFS spectrum at the Pd K-edge of the recycled catalyst (Figure 12; Table 2, entry 6) showed the presence of palladium particles ($N_{Pd-Pd} = 6$) interacting with oxygen atoms at a shorter distance than that observed in Rh(cod)-Pd/SiO_2 (Table 2, entry 4). Scheme 8 illustrates a tentative structure of the quenched and air-exposed sample.

The next step was to use the first-recycle, air-treated catalyst in a second catalytic reaction. After 24 h, the reaction was terminated, yielding 68% conversion, and the catalyst was transferred into the EXAFS sample holder under argon in a drybox. The Rh K-edge spectrum showed a rhodium center surrounded by two phosphorus atoms and four C atoms (Table 1, entry 9; Figure 11). A contribution from palladium surface atoms of adjacent metal particles was again detected. The determination of an average contribution of four C atoms, instead of the expected six as found at 33% benzene conversion (Table 1, entry 7), may be due to the presence of different species onto the quenched catalyst that was actually subjected to a remarkable chemical stress (first catalysis run at 33% conversion/aging in the air/second catalysis run for 24 h/recovery under argon). Indeed, the spectrum at the Pd K-edge of this sample (Figure 12; Table 2, entry 7) showed a significant increase in the average size of the palladium particles ($d_{mean} =$ 30 Å) with respect to the value measured prior to the exposure to air. Such a particle enlargement is typical of palladium catalysts subjected to repeated hydrogenation cycles.[37] Consistent with the magnitude of the metal particles, no appreciable oxygen contribution was detected.

Carbonylation reactions were carried in the DRIFTS apparatus for all samples, prior to and after repeated catalysis cycles, with or without air exposure. The treatment of all samples with CO regenerated the dicarbonyl $[Rh(CO)_2(dppp)]^+$, thus confirming the excellent stability of the electrostatically tethered $[Rh(dppp)]^+$ moiety even when subjected to repeated severe treatments.

Overall, the EXAFS and DRIFTS data are fully consistent with a remarkable chemical stability of the anchored $[Rh(dppp)]^+$ single sites and suggest that the catalytic activity enhancement observed with the recycled/air-exposed catalysts may really be due to a restructuring of the Pd particle surface.[32] Besides oxidation/reduction cycles, a role in the surface modification process may also be played by the $[Rh(dppp)]^+$ fragments through the formation of structures of the type shown in Scheme 8.

Proposed Catalytic Mechanism. Scheme 9 illustrates a mechanism for the hydrogenation of benzene by Rh(cod)-Pd/SiO_2 that we propose on the basis of the experimental evidence accumulated in this work. First of all, we are confident to state that the much faster hydrogenation rate of Rh(cod)-Pd/SiO_2 as compared to Pd/SiO_2 is due to the combined action of the rhodium single sites and of the surface palladium atoms on the substrate. In particular, the contribution of palladium is mandatory for the conversion of benzene to cyclohexa-1,3-diene, yet the hydrogenation of the latter requires the action of the rhodium complex to be fast and irreversible. The overall mechanism comprises three distinct reaction paths that reflect the concomitant presence on the support material of chemically interacting Rh^I single sites and palladium nanoparticles (a), isolated palladium nanoparticles (b), and isolated Rh^I single sites (c).

Overall, the present mechanism is rather similar to that previously suggested for benzene hydrogenation by Rh(cod)-(sulfos)-Pd/SiO_2 catalysis, shown in Scheme 10.[2] However, some specific differences exist.

For example, the hydrogenation of cyclohexa-1,3-diene to cyclohexane has been described in Scheme 9 as occurring with the exclusive assistance of the rhodium single sites with no involvement of the palladium particles. Obviously, this is an extreme representation of the actual process, as no one can rule out that an interaction between the rhodium sites and the palladium atoms may persist under catalytic conditions; however, it is a fact that Rh(cod)/SiO_2 is much more active than Rh(cod)-Pd/SiO_2 for the hydrogenation of cyclohexa-1,3-diene to cyclohexane. Moreover, the largely prevalent proportion of all-cis cyclohexane (stereoselective H_2 cis-additions) in the reduction of C_6H_6-d_6 with H_2 on Rh(cod)-Pd/SiO_2, as compared to Pd/SiO_2, corroborates the hypothesis that the reduction of cyclohexa-1,3-diene to cyclohexane is prevalently assisted by the Rh^I sites.

It is noteworthy that no evidence for the decoordination of a phosphine arm of dppp was obtained at any stage of the reactions catalyzed by Rh(cod)-Pd/SiO_2, whereas phosphine arm unfastening was actually required by Rh(cod)(sulfos)-Pd/SiO_2 for substrate activation and first H_2 uptake (Scheme 10).[2] This difference as well as the fact that, unlike $[Rh(sulfos)]^+$, the $[Rh(dppp)]^+$ fragment is able to pick up a benzene molecule can well account for the higher activity of Rh(cod)-Pd/SiO_2 vs Rh(cod)(sulfos)-Pd/SiO_2.[2]

(37) Grunes, J.; Zhu, J.; Somorjai, G. A. In *Nanotechnology in Catalysis*; Zhou, B., Hermans, S., Somorjai, G. A., Eds.; Springer: Berlin, 2004; Vol. 1, Chapter 1.

Concluding Remarks

This paper describes the synthesis and characterization of an unprecedented type of hybrid bimetallic catalyst that combines silica-supported palladium nanoparticles with an electrostatically anchored rhodium complex. As such, this synthetic method can extended to any cationic metal complex with no modification of the primitive molecular structure of the ligand, provided the counteranion is able to form H-bonds to the support material holding the metal particles.

The product obtained from the H-bond/ionic immobilization of [Rh(cod)(dppp)]OTf onto Pd/SiO_2 has been employed to catalyze the hydrogenation of benzene to cyclohexane, showing much higher activity as compared to Pd/SiO_2, even at extremely low rhodium loading. In situ and ex situ EXAFS and DRIFTS measurements, batch catalytic reactions under different conditions, deuterium labeling experiments, and model organometallic studies, taken altogether, have provided valuable information on the mechanism by which the rhodium single sites and the palladium nanoparticles cooperate with each other in promoting the hydrogenation of benzene. The combined action of the two metals activates the arene so as to allow the rhodium sites to enter the catalytic cycle and speed up the overall hydrogenation process by rapidly reducing benzene to cyclohexa-1,3-diene.

The new hybrid catalyst exhibits an excellent stability to repeated catalysis cycles with no need of careful handling, which contrasts with the intrinsic instability of the $[Rh(dppp)]^+$ fragment under homogeneous hydrogenation conditions. The formation of Rh−O bonds involving oxygen atoms from either the silica support or oxidized Pd particles has been identified as the factor that stabilizes the Rh single sites. Notably, the exposure to air of used catalysts has a beneficial effect on the hydrogenation activity, which may be due to the modification of the Pd particle surface by the oxidation/reduction cycles as well as the formation of (dppp)Rh−O−Pd(surface) bonds.

The present protocol for tethered complexes on supported metals can provide a number of innovative hybrid catalysts with various applications, including stereoselective reactions provided chiral metal complexes and/or chiral modifiers of metal surfaces are used.

Acknowledgment. The ELETTRA synchrotron light laboratory in Basovizza (Trieste, Italy) and the staff of the XAFS beamline are gratefully acknowledged for their support and technical assistance. We thank also the Ministry of University and Research of Italy (MUR) for financial support (FISR project: Nanosistemi inorganici ed ibridi per lo sviluppo e l'innovazione di celle a combustibile) and the European Commission for financing the Network of Excellence IDECAT (contract no. NMP3-CT-2005-011730).

OM800223D